Self-oligomerization regulates stability of survival motor neuron protein isoforms by sequestering an SCF^{Slmb} degron

Kelsey M. Gray[a,b], Kevin A. Kaifer[c], David Baillat[d], Ying Wen[b], Thomas R. Bonacci[a,e], Allison D. Ebert[f], Amanda C. Raimer[a,b], Ashlyn M. Spring[b], Sara ten Have[g], Jacqueline J. Glascock[c], Kushol Gupta[h], Gregory D. Van Duyne[h], Michael J. Emanuele[a,e], Angus I. Lamond[g], Eric J. Wagner[d], Christian L. Lorson[c], and A. Gregory Matera[a,b,*]

[a]Curriculum in Genetics and Molecular Biology and Lineberger Comprehensive Cancer Center, [b]Integrative Program in Biological and Genome Sciences, Department of Biology and Department of Genetics, and [e]Department of Pharmacology, University of North Carolina, Chapel Hill, NC 27599; [c]Molecular Pathogenesis and Therapeutics Program, Department of Veterinary Pathobiology, College of Veterinary Medicine, University of Missouri, Columbia, MO 65211; [d]Department of Biochemistry and Molecular Biology, University of Texas Medical Branch, Galveston, TX 77550; [f]Department of Cell Biology, Neurobiology and Anatomy, Medical College of Wisconsin, Milwaukee, WI 53226; [g]Centre for Gene Regulation and Expression, School of Life Sciences, University of Dundee, Dundee DD15EH, UK; [h]Department of Biochemistry and Biophysics, Perelman School of Medicine at the University of Pennsylvania, Philadelphia, PA 19104

ABSTRACT **Spinal muscular atrophy (SMA) is caused by homozygous mutations in human *SMN1*. Expression of a duplicate gene (*SMN2*) primarily results in skipping of exon 7 and production of an unstable protein isoform, SMNΔ7. Although *SMN2* exon skipping is the principal contributor to SMA severity, mechanisms governing stability of survival motor neuron (SMN) isoforms are poorly understood. We used a *Drosophila* model system and label-free proteomics to identify the SCF^{Slmb} ubiquitin E3 ligase complex as a novel SMN binding partner. SCF^{Slmb} interacts with a phosphor degron embedded within the human and fruitfly SMN YG-box oligomerization domains. Substitution of a conserved serine (S270A) interferes with SCF^{Slmb} binding and stabilizes SMNΔ7. SMA-causing missense mutations that block multimerization of full-length SMN are also stabilized in the degron mutant background. Overexpression of SMNΔ7^{S270A}, but not wild-type (WT) SMNΔ7, provides a protective effect in SMA model mice and human motor neuron cell culture systems. Our findings support a model wherein the degron is exposed when SMN is monomeric and sequestered when SMN forms higher-order multimers.**

Monitoring Editor
Yukiko Yamashita
University of Michigan

Received: Nov 7, 2017
Accepted: Nov 14, 2017

INTRODUCTION

Spinal muscular atrophy (SMA) is a common neuromuscular disorder, recognized as the most prevalent genetic cause of early childhood mortality (Pearn, 1980). Patients with the most severe form of the disease, which is also the most common, become symptomatic in the first 6 mo of life and rarely live past 2 yr (Prior, 2010; Wee *et al.*, 2010). Because the onset of symptoms and their severity can vary, SMA has historically been classified into three subtypes (Ogino and Wilson, 2004). More recently, clinicians have recognized that SMA is better characterized as a continuous spectrum disorder, ranging from acute (prenatal onset) to nearly asymptomatic (Tiziano *et al.*, 2013). Clinically, SMA patients experience degeneration of motor neurons in the anterior horn of the lower spinal cord (Crawford and Pardo, 1996). This leads to progressive atrophy of proximal muscle groups, ultimately resulting in loss of motor function and symmetrical paralysis. The cause of death is often restrictive respiratory failure (Kolb and Kissell, 2015).

SMA typically results from homozygous deletion of the *survival motor neuron 1* (*SMN1*) gene (Lefebvre *et al.*, 1995). A small fraction

This article was published online ahead of print in MBoC in Press (http://www.molbiolcell.org/cgi/doi/ 10.1091/mbc.E17-11-0627) on November 22, 2017.

*Address correspondence to: A. Gregory Matera (matera@unc.edu).

Abbreviations used: AAV9, adeno-associated virus serotype 9; Ben, Bendless; Cul1, Cullin1; iPSC, induced pluripotent stem cells; NMJ, neuromuscular junction; S2, Schneider 2; SkpA, Skp1-related A; Slmb, supernumerary limbs; SMA, spinal muscular atrophy; SMN, survival motor neuron; UPS, ubiquitin proteasome system.

© 2018 Gray *et al.* This article is distributed by The American Society for Cell Biology under license from the author(s). Two months after publication it is available to the public under an Attribution–Noncommercial–Share Alike 3.0 Unported Creative Commons License (http://creativecommons.org/licenses/by-nc-sa/3.0).
"ASCB®," "The American Society for Cell Biology®," and "Molecular Biology of the Cell®" are registered trademarks of The American Society for Cell Biology.

of SMA patients have lost one copy of *SMN1* and the remaining copy contains a point mutation (Burghes and Beattie, 2009). Humans have two *SMN* paralogues, named *SMN1* and *SMN2*, both of which contribute to total cellular levels of survival motor neuron (SMN) protein. *SMN2* exon 7 contains a silent base change that alters splicing to primarily produce a truncated, unstable protein product called SMNΔ7 (Lorson *et al.,* 1999; Monani *et al.,* 1999; Lorson and Androphy, 2000). The last 16 amino acids of SMN are replaced in SMNΔ7 by four amino acids, EMLA, encoded by exon 8. Current estimates suggest that *SMN2* produces 10–15% of the level of full-length protein produced by *SMN1* (Lorson *et al.,* 2010). Complete loss of SMN is lethal in all organisms investigated to date (O'Hearn *et al.,* 2016). Although the amount of full-length protein produced by *SMN2* is not enough to compensate for loss of *SMN1*, *SMN2* is sufficient to rescue embryonic lethality (Monani *et al.,* 2000). SMA is therefore a disease that arises due to a hypomorphic reduction in SMN levels (Lefebvre *et al.,* 1995). Furthermore, relative levels of the SMN protein correlate with the phenotypic severity of SMA (Coovert *et al.,* 1997; Lefebvre *et al.,* 1997).

Whereas a causative link between *SMN1* and SMA was established in the early 1990s, the molecular role of SMN in disease etiology remains unclear. SMN is the central component of a multimeric protein assemblage known as the SMN complex (Li *et al.,* 2014; Matera and Wang, 2014). The best-characterized function of this complex, which is found in all tissues of metazoan organisms, is in the cytoplasmic assembly of small nuclear ribonucleoproteins (snRNPs), core components of the spliceosome (Fischer *et al.,* 1997; Meister *et al.,* 2001; Pellizzoni *et al.,* 2002).

Although it is ubiquitously expressed, SMN has also been implicated in a number of tissue-specific processes related to neurons and muscles. These functions include actin dynamics (Oprea *et al.,* 2008; Ackermann *et al.,* 2013), axonal pathfinding (Fan and Simard, 2002; McWhorter *et al.,* 2003; Sharma *et al.,* 2005), axonal transport of β-actin mRNP (Rossoll *et al.,* 2003), phosphatase and tensin homolog-mediated (PTEN-mediated) protein synthesis pathways (Ning *et al.,* 2010), translational regulation (Sanchez *et al.,* 2013), neuromuscular junction formation and function (Chan *et al.,* 2003; Kariya *et al.,* 2008; Kong *et al.,* 2009; Voigt *et al.,* 2010), myoblast fusion (Shafey *et al.,* 2005), and maintenance of muscle architecture (Rajendra *et al.,* 2007; Walker *et al.,* 2008; Bowerman *et al.,* 2009).

Ubiquitylation pathways have been shown to regulate the stability and degradation of SMN (Chang *et al.,* 2004; Burnett *et al.,* 2009; Hsu *et al.,* 2010) as well as axonal and synaptic stability (Korhonen and Lindholm, 2004). In the ubiquitin proteasome system (UPS), proteins destined for degradation are tagged by linkage to ubiquitin through the action of three factors (Petroski, 2008). E1 proteins activate ubiquitin and transfer it to the E2 enzyme. E2 proteins conjugate ubiquitin to their substrates. E3 proteins recognize the substrate and assist in the transfer of ubiquitin from the E2. Because E3 ligases confer substrate specificity, they are typically considered as candidates for targeted inhibition of protein degradation. Ubiquitin homeostasis is thought to be particularly important for neuromuscular pathology in SMA (Groen and Gillingwater, 2015). Indeed, mouse models of SMA display widespread perturbations in UBA1 (ubiquitin-like modifier activating enzyme 1) levels (Wishart *et al.,* 2014). Furthermore, mutations in UBA1 are known to cause X-linked infantile SMA (Ramser *et al.,* 2008; Schmutzler *et al.,* 2008).

Given the importance of these processes to normal development as well as neurodegenerative disease, we set out to identify and characterize novel SMN binding partners. Previously, we developed *Drosophila melanogaster* as a model system wherein the endogenous *Smn* gene is replaced with a *Flag-Smn* transgene (Praveen *et al.,* 2012). Although it is highly similar to human *SMN1* and *SMN2*, the entire open reading frame of fruitfly *Smn* is contained within a single exon, and so only full-length SMN protein is expressed in *Drosophila* (Rajendra *et al.,* 2007). When modeled in the fly, SMA-causing point mutations recapitulate the full range of phenotypic severity seen in humans (Praveen *et al.,* 2014; Garcia *et al.,* 2016). Using this system, we carried out proteomic profiling of Flag-purified embryonic lysates and identified the SCF^{Slmb} E3 ubiquitin ligase complex as a novel SMN interactor. Importantly, this interaction is conserved from flies to humans. We show that SCF^{Slmb} binding requires a phosphodegron motif located within the SMN self-oligomerization domain, mutation of which stabilizes SMNΔ7 and, to a lesser extent, full-length SMN. Additional studies in flies, mice, and human cells elucidate a disease-relevant mechanism whereby SMN protein stability is regulated by self-oligomerization. Other E3 ligases have been reported to target SMN for degradation in cultured human cells (Hsu *et al.,* 2010; Kwon *et al.,* 2013; Han *et al.,* 2016). Given our findings in fruit-fly embryos, SMN is likely targeted by multiple E3 ubiquitin ligases.

RESULTS

Flag-SMN interacts with ubiquitin proteasome system proteins

We previously generated transgenic flies that express Flag-tagged SMN proteins in an otherwise null *Smn* background (Praveen *et al.,* 2012). To preserve endogenous expression patterns, the constructs are driven by the native promoter and flanking sequences. As described under *Materials and Methods*, we intercrossed hemizygous $Flag\text{-}Smn^{WT}$,Smn^{X7}/Smn^{D} animals to establish a stock wherein all of the SMN protein, including the maternal contribution, is epitope tagged. After breeding them for >100 generations, essentially all of the animals are homozygous for the $Flag\text{-}Smn^{WT}$ transgene, but second-site recessive mutations are minimized due to the use of two different *Smn* null alleles. Adults from this stock display no apparent defects and have an eclosion frequency (~90%) similar to that of wild-type (Oregon-R) animals.

We collected (0–12 h) embryos from $Flag\text{-}Smn^{WT/WT}$,$Smn^{X7/D}$ (SMN) and Oregon-R (Ctrl) animals and analyzed Flag-purified lysates by "label-free" mass spectrometry. In addition to Flag-SMN, we identified SMN complex components Gemin2 and Gemin3, along with all seven of the canonical Sm-core snRNP proteins (Figure 1A). We also identified the U7-specific Sm-like heterodimer Lsm10/11 (Pillai *et al.,* 2003) and the Gemin5 orthologue, Rigor mortis (Gates *et al.,* 2004). Previous studies of Schneider2 (S2) cells transfected with epitope-tagged *Smn* had identified most of the proteins listed above as SMN binding partners in *Drosophila* (Kroiss *et al.,* 2008). However, despite bioinformatic and cell biological data indicating that Rigor mortis is part of the fruit-fly SMN complex, this protein failed to copurify with SMN in S2 cells (Kroiss *et al.,* 2008; Cauchi *et al.,* 2010; Guruharsha *et al.,* 2011). On the basis of our purification data, we conclude that the conditions are effective and that Rigor mortis/Gemin5 is an integral member of the SMN complex in flies.

A detailed proteomic analysis of these flies will be presented elsewhere. As shown in Figure 1B, our preliminary analysis identified 396 proteins, 114 of which were detected only in the Flag-SMN sample and not in the control. An additional 279 proteins were detected in both the Flag purification and control samples. In addition to SMN complex members, we copurified numerous factors that are part of the ubiquitin proteasome system (UPS; Figure 1C). Among these UPS proteins, we identified Cullin 1 (Cul1), Skp1-related A (SkpA), and supernumerary limbs (Slmb), as being highly enriched

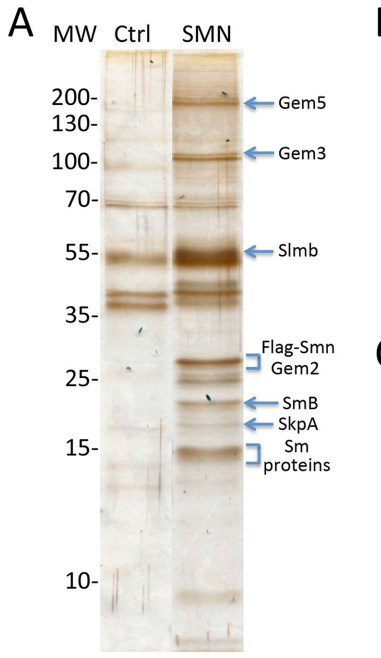

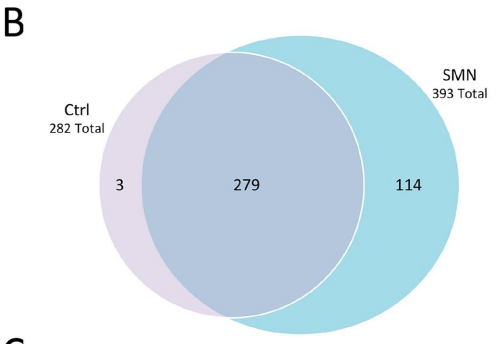

C

Protein	Gene #	Category	Intensity Ctrl (x10^5)	Intensity SMN (x10^5)	Peptides
Known SMN Interactors					
SMN	CG16725	SMN Complex	38.7	1415.2	9
Gem3	CG6539	SMN Complex	31.0	1052.2	31
Gem2	CG10419	SMN Complex	0.0	372.6	5
Gem5	CG30149	SMN Complex	0.0	96.5	16
SmE	CG18591	Sm protein	0.9	439.8	3
SmG	CG9742	Sm protein	0.4	364.5	6
SmD2	CG1249	Sm protein	0.0	303.4	5
SmF	CG16792	Sm protein	0.0	89.9	4
Lsm11	CG12924	Sm protein	0.0	47.3	8
SmD3	CG8427	Sm protein	0.3	31.1	2
SmD1	CG10753	Sm protein	0.0	20.0	3
SmB	CG5352	Sm protein	0.0	13.3	1
Lsm10	CG12938	Sm protein	0.0	11.2	2
Select Candidates					
Slmb	CG3412	UPS - SCF E3	0.7	253.6	13
SkpA	CG16983	UPS - SCF E3	3.4	91.1	5
Ben	CG18319	UPS - E2	2.1	27.3	5
Ubc2	CG6720	UPS - E2	2.9	9.2	2
Cul1	CG1877	UPS - SCF E3	0.0	8.0	4
UBE2S-like	CG8188	UPS - E2	0.0	5.8	3
Uch-L5	CG3431	UPS - DUB	1.1	4.5	2
Hyd	CG9484	UPS - E3	0.0	3.6	2
Cul5	CG1401	UPS - E3	0.0	2.8	2
Rpt1	CG1341	Proteasome	12.9	31.1	7
Rpt4	CG3455	Proteasome	8.8	29.2	6
Rpn2	CG11888	Proteasome	11.0	28.6	5
Rpn9	CG10230	Proteasome	6.5	23.0	5
Rpn6	CG10149	Proteasome	11.2	21.5	4
Rpn3	CG42641	Proteasome	2.7	15.3	5
Rpt3	CG16916	Proteasome	5.4	14.6	5
Rpn5	CG1100	Proteasome	6.0	13.2	4
Rpn11	CG18174	Proteasome	2.5	13.0	2
Rpn1	CG7762	Proteasome	1.9	11.0	5
Rpn7	CG5378	Proteasome	2.8	7.6	2
Rpn12	CG4157	Proteasome	2.5	5.2	3
CSN7	CG2038	COP9 signalosome	0.8	5.4	3
CSN3	CG18332	COP9 signalosome	0.0	3.7	2
CSN4	CG8725	COP9 signalosome	0.0	2.9	2
Sgg	CG2621	Kinase	2.2	9.8	4

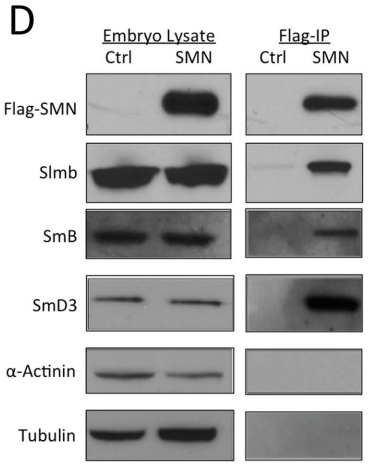

FIGURE 1: Flag-SMN immunopurified lysates contain known protein interaction partners and ubiquitin proteasome system (UPS) proteins. (A) Lysates from Oregon-R control (Ctrl) *Drosophila* embryos and embryos expressing only transgenic Flag-SMN (SMN) were Flag-immunopurified, and protein eluates were separated by gel electrophoresis and silver stained. Band identities predicted by size using information from panels C and D. (B) Direct mass spectrometric analysis of the eluates (which were not gel purified) identified a total of 396 proteins, 114 of which were detected only in SMN sample and 279 of which were detected in both SMN and Ctrl samples. (C) Flag-purified eluates were analyzed by "label-free" mass spectrometry. Numerous proteins that copurify with Flag-SMN are part of the ubiquitin proteasome system (UPS). Of these UPS proteins, Cullin 1 (Cul 1), SkpA, and supernumerary limbs (Slmb) were highly enriched (at least 10-fold) in the SMN sample as compared with Ctrl. (D) Western blot analysis of Flag-purified eluates was used to further validate the presence or absence of SMN interaction partners. Flag-SMN was successfully purified from SMN embryos but was undetectable in the control. As positive controls for known protein interaction partners of SMN, SmB and SmD3 were also easily detectable by Western blotting using anti-Sm antibodies. The presence of Slmb was verified using anti-Slmb. α-Actinin and tubulin were not enriched in our purification and are used as negative controls to demonstrate specificity.

(>10-fold) in Flag-SMN samples as compared with the control. Together, these proteins comprise the SCF^{Slmb} E3 ubiquitin ligase. Cul1 forms the major structural scaffold of this horseshoe-shaped, multisubunit complex (Zheng *et al.*, 2002). Slmb is an F-box protein and is the substrate recognition component (Jiang and Struhl, 1998). SkpA is a bridging protein essential for interaction of Cul1 with the F-box protein (Patton *et al.*, 1998a,b). Because of its role in substrate recognition, Slmb is likely to be the direct interacting partner of SMN within the SCF^{Slmb} complex. For this reason, we focused on Slmb for the initial validation. As shown, Slmb was easily detectable in Flag-purified eluates from embryos expressing Flag-SMN and nearly undetectable in those from control embryos (Figure 1D). SmB and SmD3 were also easily detectable by Western blot in Flag-purified embryonic lysates and were used as positive controls for known protein interaction partners of SMN. Tubulin and α-actinin were not detected as interacting with SMN in our purification and demonstrate the specificity of the detected SMN interactions.

SCF^{Slmb} is a bona fide SMN interaction partner that ubiquitylates SMN

As an E3 ubiquitin ligase, the SCF^{Slmb} complex is a substrate recognition component of the ubiquitin proteasome system. As outlined in Figure 2A, E3 ligases work with E1 and E2 proteins to ubiquitylate their targets. The interaction of SCF^{Slmb} with SMN was verified in a reciprocal coimmunoprecipitation, demonstrating that Flag-tagged SCF components form complexes with endogenous SMN (Figure 2B) in S2 cells.

SCF complexes are highly conserved from flies to humans: SkpA is 77% identical to human Skp1, Cul1 is 63% identical, and Slmb is 80% identical to its human homologues, B-TrCP1 and B-TrCP2. Slmb/B-TrCP is the SCF component that directly contacts substrates of the E3 ligase. We therefore tested the interaction of recombinant human SMN in complex with (SMN•Gem2) Gupta *et al.*, 2015) with glutathione *S*-transferase (GST)-tagged B-TrCP1 and -SMN proteins in an in vitro binding assay. As shown in Figure 2C, SMN•Gem2 did not interact with GST alone but was detected at high levels following pull down with either GST-SMN (positive control) or GST-B-TrCP1. We also tested the interaction of Flag-tagged *Drosophila* SCF components with endogenous human SMN in HEK 293T cells (Figure 2D). Accordingly, human SMN was coprecipitated with Flag-Cul1 and Flag-Slmb and at lower levels following Flag-SkpA immunoprecipitation. Flag-B-TrCP1 and Flag-B-TrCP2, the two human homologues of Slmb, also copurified with endogenous human SMN in HEK 293T cells (Figure 2E). Altogether, these data demonstrate a conserved interaction between SMN and the SCF$^{Slmb/B\text{-}TrCP}$ E3 ubiquitin ligase complex.

To test the functional consequences of this conserved interaction between SMN and SCF$^{Slmb/B\text{-}TrCP}$, a cell-based ubiquitylation assay

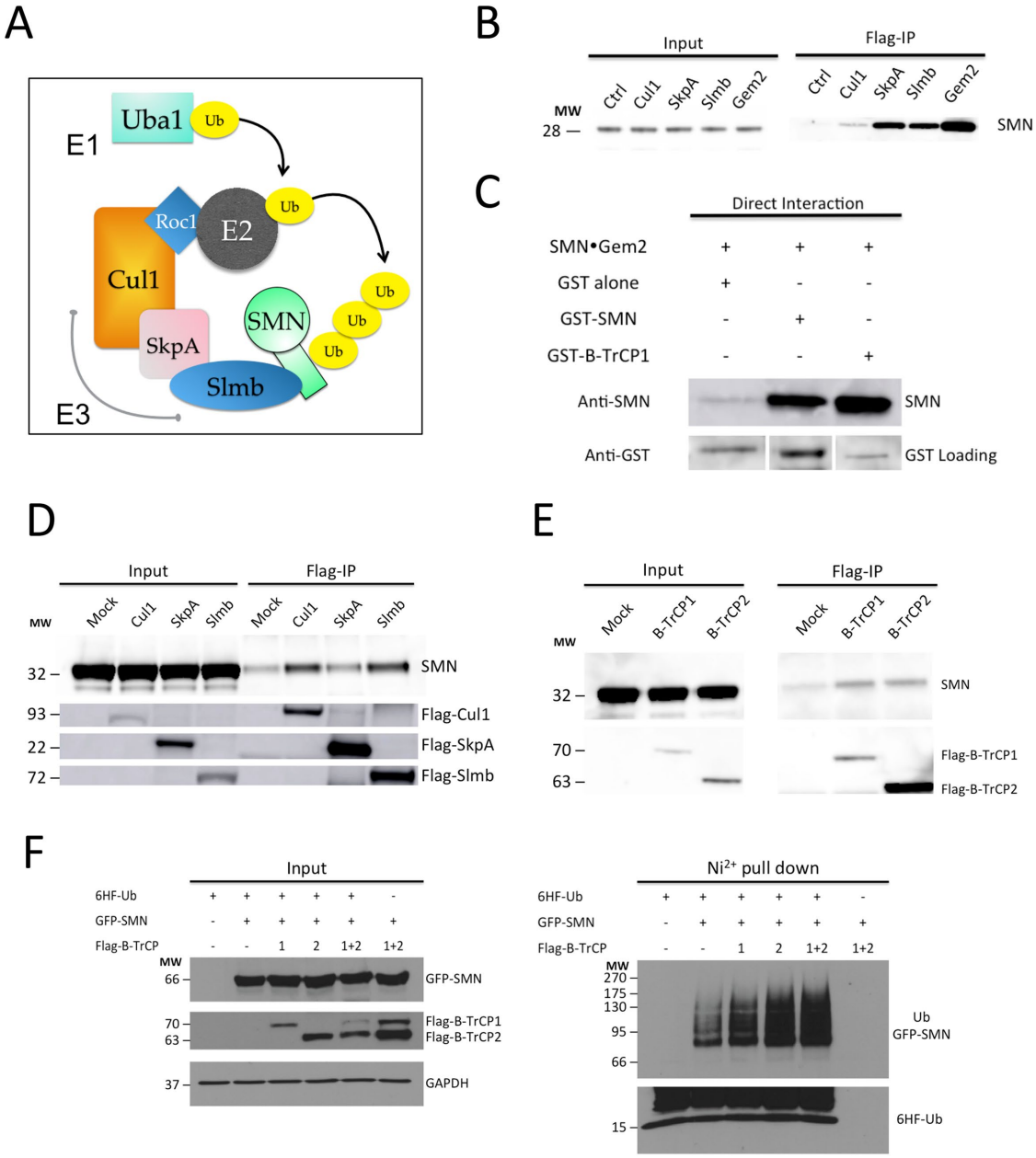

FIGURE 2: Conserved interaction between SMN and the $SCF^{Slmb/B\text{-}TrCP}$ E3 ubiquitin ligase results in ubiquitylation of SMN. (A) E3 ligases work with E1 and E2 proteins to ubiquitylate their targets. The $SCF^{Slmb/B\text{-}TrCP}$ E3 ubiquitin ligase is made up of three proteins: Cul1, SkpA, and Slmb. The E3 ubiquitin ligase is the substrate recognition component of the ubiquitin proteasome system. (B) Following Cul1-Flag, SkpA-Flag, Flag-Slmb, and Flag-Gem2 immunoprecipitation from *Drosophila* S2 cell lysates, Western analysis using anti-SMN antibody for endogenous SMN was carried out. Copurification of each of the SCF components with endogenous SMN was detected. (C) An in vitro binding assay tested direct interaction between human SMNΔ5-Gemin2 (SMN•Gem2) (Martin *et al.*, 2012; Gupta *et al.*, 2015) and purified GST-tagged proteins. SMN•Gem2 did not interact with GST protein alone but bound to GST tagged *Drosophila* SMN (GST-SMN) and GST tagged human B-TrCP1 (GST-B-TrCP1). Levels of GST alone, GST-SMN, and GST-B-TrCP1 were detected using anti-GST antibody. (D) The interaction of Flag-tagged *Drosophila* SCF components with endogenous human SMN was tested in in HEK 293T cells. Human SMN was detected at high levels following immunoprecipitation of Drosophila Flag-Cul1 and Flag-Slmb and detected at a lower level following Drosophila Flag-SkpA immunoprecipitation. (E) Flag-tagged versions of the human homologues of Slmb, Flag-B-TrCP1, and Flag-B-TrCP2, interact with endogenous human SMN in HEK 293T cells demonstrated by Flag-immunopurification followed by immunodetection of SMN. (F) Protein lysate from HEK 293T cells transfected with 6xHis-Flag-ubiquitin (6HF-Ub) and GFP-SMN was purified using a Ni^{2+} pull down for the tagged ubiquitin. Baseline levels of ubiquitylated GFP-SMN were detected using anti-GFP antibody. Following transfection of Flag-B-TrCP1 or Flag-B-TrCP2, the levels of ubiquitylated SMN markedly increased. Ubiquitylation levels were further increased following addition of both proteins together. In the input, GFP-SMN was detected using anti-GFP antibody, Flag-B-TrCP1 and Flag-B-TrCP2 were detected using anti-Flag antibody, and GAPDH was detected by anti-GAPDH antibody. In the Ni^{2+} pull down, ubiquitylated GFP-SMN was detected using anti-GFP antibody and 6HF-Ub was detected using anti-Flag antibody to verify successful pull down of tagged ubiquitin.

was performed (Figure 2F). Protein lysate from HEK 293T cells transfected with 6xHis-Flag-ubiquitin and GFP-SMN was purified using a Ni^{2+} pull down for the tagged ubiquitin. Baseline levels of ubiquitylated GFP-SMN were detected using anti-GFP antibody. Following transfection of Flag-B-TrCP1 or Flag-B-TrCP2, the levels of ubiquitylated SMN markedly increased (Figure 2F). Ubiquitylation levels were further increased following addition of both proteins together. These experiments demonstrate that $SCF^{Slmb/B\text{-}TrCP}$ can ubiquitylate SMN in vivo.

Depletion of Slmb/B-TrCP results in a modest increase in SMN levels

Given that one of the primary functions of protein ubiquitylation is to target proteins to the proteasome, we examined whether depletion of Slmb by RNA interference (RNAi) using double-stranded RNA (dsRNA) in S2 cells would increase SMN levels (Figure 3A). Following Slmb RNAi, endogenous SMN levels were modestly increased as compared with cells treated with control dsRNA. We obtained similar results using an siRNA that targets both B-TrCP1 and B-TrCP2 in HeLa cells. As shown in Figure 3B, we detected a modest increase in levels of full-length SMN following B-TrCP RNAi but not control RNAi. Next, we treated S2 cells with cycloheximide (CHX), in the presence or absence of dsRNA targeting Slmb, to determine whether differences in SMN levels would be exacerbated when production of new proteins was prevented (Figure 3C). SMN protein levels were also specifically targeted using dsRNA against *Smn* as a positive control for the RNAi treatment. At 6 h post–CHX treatment, there was a modest increase in full-length SMN levels following Slmb RNAi as compared with the initial timepoint (0 h) or the negative control (Ctrl) RNAi (Figure 3C). Together, these data indicate that Slmb/B-TrCP participates in the regulation of SMN protein levels.

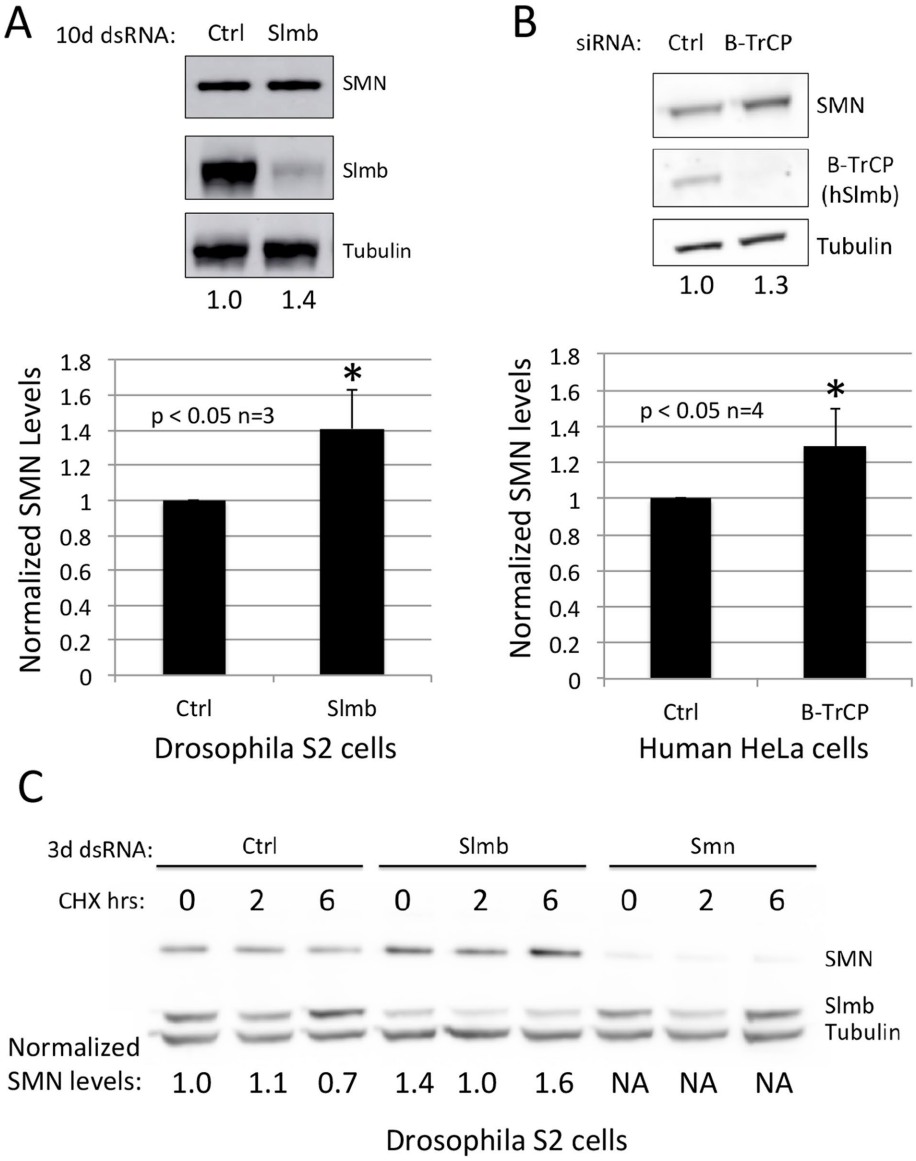

FIGURE 3: Depletion of Slmb/B-TrCP results in an increase of SMN levels. (A) Depletion of Slmb using 10-d (10d) treatment with dsRNA in *Drosophila* S2 cells resulted in modestly increased SMN levels. Following Slmb RNAi, full-length SMN levels were increased as compared with cells treated with control dsRNA against Gaussia Luciferase, which is not expressed in S2 cells. (B) The effect of B-TrCP depletion on SMN levels in human cells was tested using siRNA that targets both B-TrCP1 and B-TrCP2 in HeLa cells. We detected a modest increase in levels of full-length endogenous SMN after B-TrCP RNAi but not control (scramble) RNAi. (C) *Drosophila* S2 cells were treated with cycloheximide (CHX), an inhibitor of protein synthesis, following Slmb depletion following a 3-d dsRNA treatment to test whether differences in protein levels would be exacerbated when the production of new protein was prevented. SMN protein levels were also directly targeted using dsRNA against *Smn* as a positive control for the RNAi treatment. As a negative control (Ctrl), dsRNA against *oskar*, which is not expressed in S2 cells, was used. Protein was collected at 0, 2, and 6 h post–CHX treatment. At 6 h post–CHX treatment, there is a modest increase in full-length SMN levels following *Slmb* RNAi as compared with the initial time point (0 h) and as compared with control RNAi treatment.

Identification and characterization of a Slmb/B-TrCP degradation signal in SMN

Studies of numerous UPS substrates in a variety of species have revealed the presence of degradation signals (called degrons) that are required for proper E3 target recognition and binding. Slmb/B-TrCP canonically recognizes a consensus DpSGXXpS/T degron, where p indicates a phosphoryl group (Fuchs *et al.*, 2004; Jin *et al.*, 2005; Frescas and Pagano, 2008). There are also several known variants of this motif, for example, DDGFVD, SSGYFS, and TSGCSS (Kim *et al.*, 2015). As shown in Figure 4A, we identified a putative Slmb/B-TrCP degron (^{269}MSGYHT^{274}) in the highly conserved self-oligomerization domain (YG Box) of human SMN. Interestingly, this sequence was previously identified as part of a larger degron motif (^{268}YMSGYHTGYYMEMLA^{282}) that was thought to be created in SMNΔ7 by *SMN2* alternative splicing (Cho and Dreyfuss, 2010). In particular, mutation of S270 (S201 in flies) to alanine was shown to dramatically stabilize SMNΔ7 constructs in human cells, and overexpression of $SMN\Delta7^{S270A}$ in SMN-deficient chicken DT40 cells rescued their viability

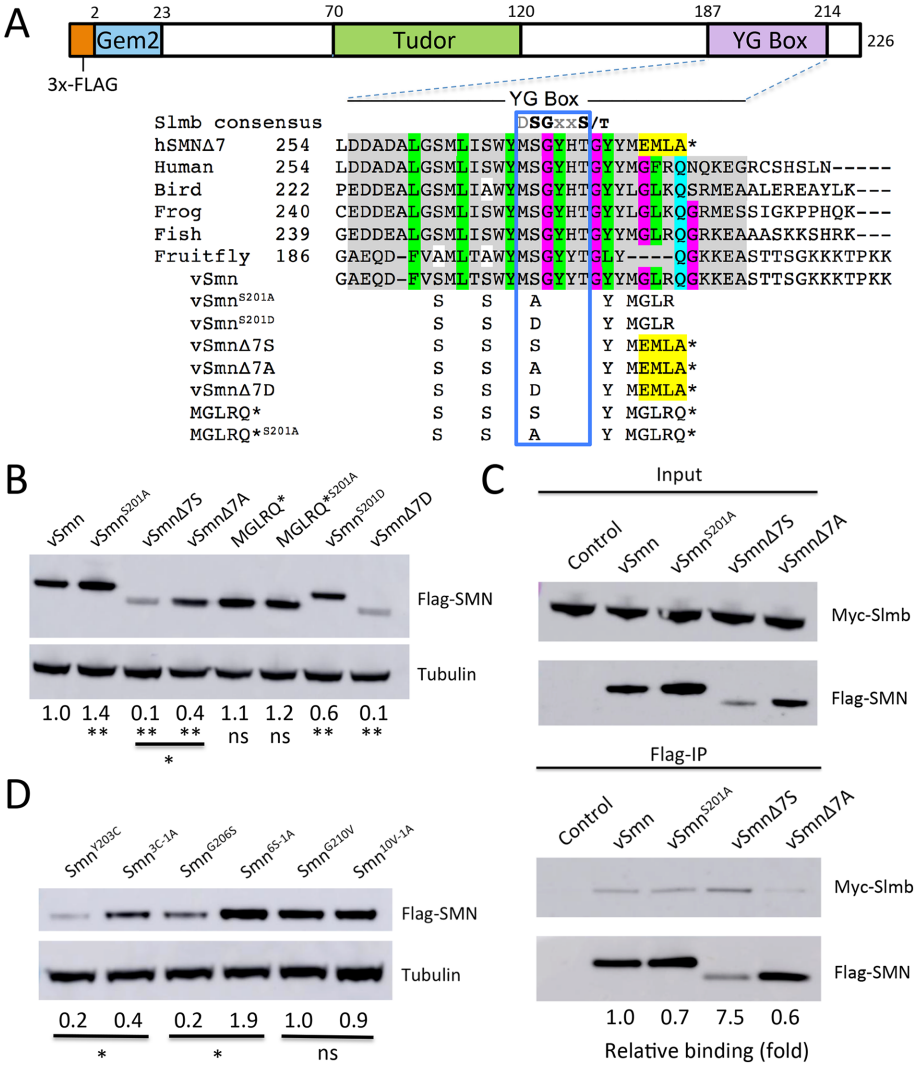

FIGURE 4: Identification and mutation of a putative Slmb/B-TrCP phosphodegron (A) Identification of a conserved putative Slmb phosphodegron (DpSGXXpS/T motif variant) in the C-terminal self-oligomerization domain (YG Box) of SMN. The amino acid sequence of SMN from a variety of vertebrates is shown to illustrate conservation of this motif and rationale for the amino acid changes. Full-length human SMN is labeled as "Human," and the truncated isoform is labeled "hSMNΔ7." Endogenous *D. melanogaster* SMN is labeled "Fruitfly." To generate a more vertebrate-like SMN, key amino acids in *Drosophila* SMN were changed to amino acids conserved in vertebrates. Using this SMN backbone, a serine-to-alanine mutation was made in the putative degron in both full-length (vSMN^{S201A}) and truncated SMNΔ7 (vSMNΔ7A). An additional SMN construct that is the same length as SMNΔ7, but has the amino acid sequence GLRQ (the next amino acids in the sequence) rather than EMLA (the amino acids introduced by mis-splicing of *SMN2*), was generated. The same serine to alanine mutation was made in this construct as well (MGLRQ* and MGLRQ*^{S201A}). Finally, to mimic a phosphorylated serine, a full-length vSmn^{S201D} and truncated vSmnΔ7D were also employed. (B) Western blotting was used to determine protein levels of each of these SMN constructs, with expression driven by the endogenous promoter, in *Drosophila* S2 cells. Both the vSMN and vSMNΔ7S proteins show increased levels when the serine is mutated to an alanine, indicating disruption of the normal degradation of SMN. Additionally, MGLRQ* protein is present at higher levels than is vSMNΔ7S and protein levels do not change when the serine is mutated to an alanine. Normalized fold change as compared with vSmn levels is indicated at the bottom. *$p < 0.05$, **$p < 0.01$, $n = 3$. (C) Flag-tagged SMN constructs were cotransfected with Myc-Slmb in *Drosophila* S2 cells. Protein lysates were Flag-immunoprecipitated and probed with anti-Myc antibody to detect SMN-Slmb interaction. In both full-length SMN (vSMN) and truncated SMN (vSMNΔ7), serine-to-alanine mutation decreased interaction of Slmb with SMN. Truncated SMN (vSMNΔ7) showed a dramatically increased interaction with Slmb as compared with full-length SMN (vSMN), despite the fact it is present at lower levels. (D) Full-length SMN constructs containing point mutations known to decrease self-oligomerization (Smn^{Y203C} and Smn^{G206S}) and a mutation that does not disrupt self-oligomerization in the fly (Smn^{G210V}) with and without the serine-to-alanine mutation were transfected in *Drosophila* S2 cells. The constructs containing the serine to alanine mutation are as follows: Smn^{Y203C}→Smn^{3C-1A}, Smn^{G206S}→Smn^{6S-1A}, Smn^{G210V}→Smn^{10V-1A}. The serine to alanine mutation has a stabilizing effect on SMN mutants with poor self-oligomerization capability. *$p < 0.05$, $n = 3$.

(Cho and Dreyfuss, 2010). However, factors responsible for specifically mediating SMNΔ7 degradation have not been identified.

To develop a more disease-relevant *Drosophila* system to investigate SMN YG box function, we generated a "vertebrate-like" SMN construct, called vSmn (Figure 4A). Transgenic flies expressing Flag-vSmn and Flag-vSmn^{S201A} in the background of an *Smn*^{X7} null mutation are fully viable (Supplemental Figure S1). In fact, the eclosion frequencies of these animals are consistently higher than those that express Flag-Smn^{WT} (Supplemental Figure S1). Additional *Smn* mutant constructs were generated using the vSmn backbone, including both the full-length (e.g., vSmn^{S201A}) and truncated (e.g., vSmnΔ7A) versions of the protein (Figure 4A). To test the effects of overall protein length and distance of the putative degron from the C-terminus, we also generated vSmn constructs that are the same length as SMNΔ7, replacing the MEMLA* motif (the amino acids introduced by human *SMN2* splicing) with MGLRQ*; see Figure 4A. The S201A mutation was created in this construct as well (MGLRQ*^{S201A}). To mimic a constitutively phosphorylated state, we also introduced serine to aspartate mutations, vSmn^{S201D} and vSmnΔ7D. We transfected each of these constructs, Flag-tagged and driven by the native *Smn* promoter, into S2 cells and measured protein levels by Western blotting (Figure 4B). We note that these constructs are expressed at levels far below those of endogenous SMN protein in S2 cells; moreover, they do not affect levels of endogenous SMN (Supplemental Figure S2). As shown, the vSmn^{S201A} and vSMNΔ7A constructs exhibited increased protein levels compared with their serine containing counterparts, whereas levels of the S201D mutants were reduced, suggesting that the phosphodegron motif identified in human SMNΔ7 (Cho and Dreyfuss, 2010) is also conserved in the fly protein. In addition to examining protein levels of each of these constructs in cell culture, transgenic flies expressing vSmn, vSmn^{S201A}, vSmnΔ7S, and vSmnΔ7A were created. Here again, we observed that the S201A mutation increased protein levels of both full-length SMN and SMNΔ7 (Supplemental Figure S3).

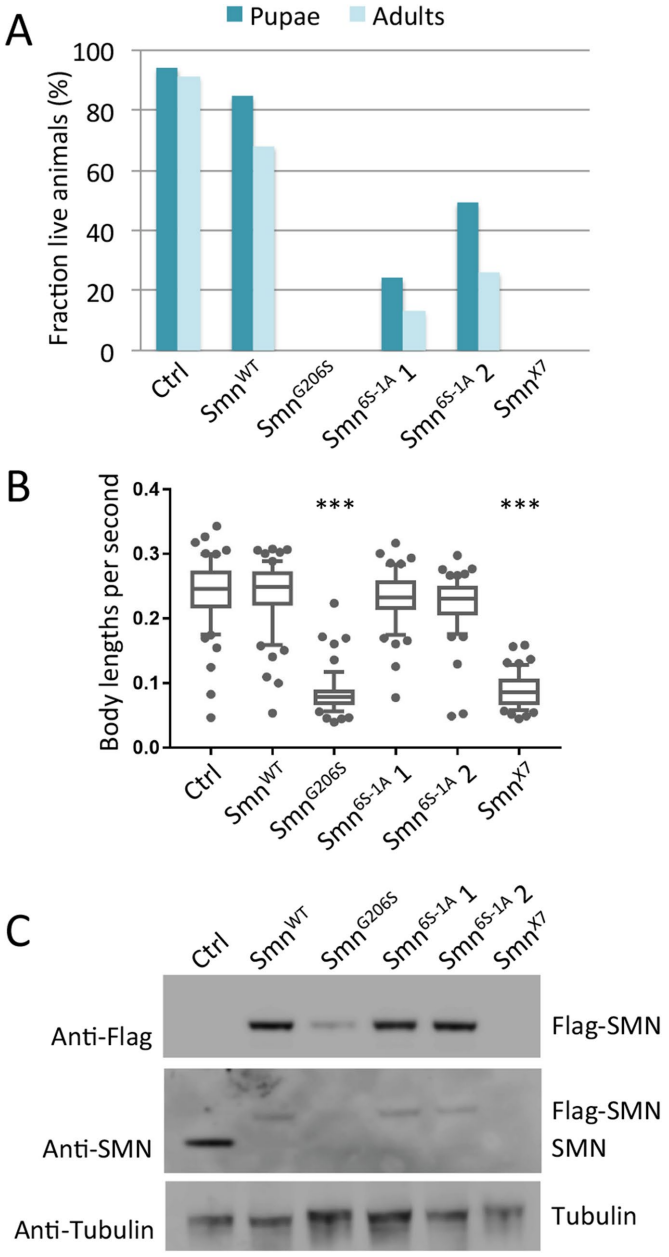

FIGURE 5: Mutation of the Slmb degron rescues defects in SMA model flies. (A) Viability analysis of an SMA point mutation (G206S) in the presence and absence of the degron mutation, S201A. Flies with the following genotypes were analyzed in this experiment: Oregon-R (Ctrl), *Flag-Smn*^{WT},*Smn*^{X7}/*Smn*^{X7} (Smn^{WT}), *Flag-Smn*^{G206S},*Smn*^{X7}/*Smn*^{X7} (Smn^{G206S}), *Flag-Smn*^{G206,S201A},*Smn*^{X7}/*Smn*^{X7} (Smn$^{6S\text{-}1A}$), or *Smn*^{X7}/*Smn*^{X7} (Smn^{X7}). The data for each genotype are expressed as a fraction of pupae or adults over the total number of starting larvae, $n = 200$. Expression of the WT transgene (*Smn*^{WT}) shows robust rescue of the null (*Smn*^{X7}) phenotype (~68% adults). *Smn*^{G206S} is a larval lethal mutation. In two independent recombinant lines of *Smn*$^{6S\text{-}1A}$ (*Smn*$^{6S\text{-}1A}$*1* and *Smn*$^{6S\text{-}1A}$*2*) a fraction of the larvae complete development to become adults. (B) Locomotor ability of early third-instar larvae was determined by tracking their movement for 1 min and then calculating the velocity. To account for potential differences in larval size, speed is expressed as average body lengths per second moved. Genotypes are as in panel A. *Smn*^{G206S} larvae move similarly to null animals. The motility of *Smn*$^{6S\text{-}1A}$*1* and *Smn*$^{6S\text{-}1A}$*2* larvae is not different from Ctrl or *Smn*^{WT} larvae. ***$p < 0.001$, $n = 50$–60 larvae. (C) Larval protein levels were examined by Western blotting; genotypes as in panel A. Lysates from hemizygous mutant lines were probed with anti-Flag or anti-SMN antibodies as indicated. The slower-migrating bands represent the Flag-tagged transgenic proteins and the faster migrating band corresponds to endogenous SMN, which is present only in the Ctrl (note Oregon-R has two copies *Smn*, whereas the transgenics have only one). *Smn*^{G206S} has very low levels of SMN protein. Flies bearing the S201A degron mutation in addition to G206S (*Smn*$^{6S\text{-}1A}$) express markedly increased levels of SMN protein.

The MGLRQ* construct is present at levels that are similar to wild type (vSmn) and much higher than vSmnΔ7S. Based on the crystal structures of the SMN YG box (Martin *et al.*, 2012; Gupta *et al.*, 2015), the presence of the MGLR insertion in *Drosophila* SMN is predicted to promote self-oligomerization (unpublished data), thus stabilizing the protein within the SMN complex (Burnett *et al.*, 2009). By the same logic, the relative inability of vSmnΔ7S to self-interact would be predicted to lead to its destruction. To determine whether the observed increase in SMN protein levels correlated with its ability to interact with Slmb, we cotransfected the appropriate Flag-Smn constructs with Myc-Slmb in S2 cells. Protein lysates were then Flag-immunoprecipitated and probed with anti-Myc antibody (Figure 4C). The S201A mutation decreased binding of Slmb to both the full-length and the truncated SMN isoforms (Figure 4C). However, the vSmnΔ7S construct coprecipitated the greatest amount of Slmb protein, despite the fact that it is present at much lower levels in the input lysate (Figure 4C). Because SMNΔ7 is defective in self-interaction, this result suggests that the degron is more accessible to Slmb when SMN is monomeric and cannot efficiently oligomerize.

SMN self-oligomerization regulates access to the Slmb degron

To examine the connection between SMN self-oligomerization and degron accessibility more closely, we took advantage of two SMA patient-derived point mutations (Y203C and G206S) that are known to destabilize the full-length protein and to decrease its self-oligomerization capacity (Praveen *et al.*, 2014). As a control, we also employed an SMA-causing mutation (G210V) that does not disrupt SMN self-oligomerization (Praveen *et al.*, 2014; Gupta *et al.*, 2015). Next, we introduced the S201A degron mutation into all three of these full-length SMN constructs, transfected them into S2 cells and carried out Western blotting (Figure 4D and Supplemental Figure S2). The S201A degron mutation has a clear stabilizing effect on the G206S and Y203C constructs, as compared with the effect of S201A paired with G210V. Hence, we conclude that the Slmb degron is exposed when SMN is present predominantly as a monomer, whereas it is less accessible when the protein is able to form higher-order multimers.

Mutation of the Slmb degron rescues viability and locomotion defects in SMA model flies

Next, we examined the effect of mutating the Slmb degron in the context of the full-length protein in vivo. We characterized adult viability, larval locomotion, and SMN protein expression phenotypes of the G206S mutants in the presence or absence of the degron mutation, S201A (Figure 5, A–C). As described previously (Praveen *et al.*, 2014), *Smn*^{G206S} animals express very low levels of SMN and fail to develop beyond larval stages. In contrast, flies bearing the S201A degron mutation in addition to G206S (*Smn*$^{6S\text{-}1A}$) express markedly increased levels of SMN protein (Figure 5C), and a good fraction of these animals complete development (Figure 5A). Moreover, *Smn*$^{6S\text{-}1A}$ larvae display significantly improved locomotor activity as compared with *Smn*^{G206S} or *Smn*^{X7} null mutants (Figure 5B).

These results strongly suggest that both the structure of the G206S mutant protein as well as its instability contribute to the organismal phenotype.

GFP-SMNΔ7 overexpression stabilizes endogenous SMN and SMNΔ7 in cultured human cells

Increased *SMN2* copy number correlates with a milder clinical phenotype in SMA patients (Oskoui *et al.*, 2016). This phenomenon was successfully modeled in mice in the early 2000s (Hsieh-Li *et al.*, 2000; Monani *et al.*, 2000), showing that high-copy-number *SMN2* transgenes fully rescue the null phenotype, whereas low-copy transgenes do not. Moreover, transgenic expression of a human *SMN*Δ7 cDNA construct in a low-copy *SMN2* background improves survival of this severe SMA mouse model from P5 (postnatal day 5) to P13 (Le *et al.*, 2005). Although the truncated SMN likely retains partial functionality, the protective effect of *SMN*Δ7 overexpression may not entirely be intrinsic to the protein. That is, SMNΔ7 could also act as a "soak-off" factor, titrating the ubiquitylation machinery and stabilizing endogenous SMN. In such a scenario, the prediction would be that SMNΔ7A is less protective than SMNΔ7S because it is not a very good substrate for SCF^{Slmb}.

We therefore compared the stabilizing effects of overexpressing GFP-tagged $SMN\Delta7^{S270A}$ (SMNΔ7A) and SMNΔ7 (SMNΔ7S) on endogenous human SMN and SMNΔ7. HEK 293T cells were transfected with equivalent amounts of GFP-SMNΔ7A or -SMNΔ7S. The following day, cells were harvested after treatment with cycloheximide (CHX) for zero to 10 h. As shown in Figure 6A, Western blotting with anti-SMN showed that the SMNΔ7S construct exhibits a clear advantage over SMNΔ7A in its ability to stabilize endogenous SMN and SMNΔ7. By comparing band intensities within a given lane, we generated average intensity ratios for each time point using replicate blots (Figure 6A, table). We then calculated a "stabilization factor" by taking a ratio of these two ratios. As shown (Figure 6A, graph), the protective benefit of overexpressing Δ7S versus Δ7A at $t = 0$ h was roughly 3.0× for endogenous SMNΔ7 and 1.75× for full-length SMN. Thus, as predicted above, the GFP-SMNΔ7A construct was much less effective at stabilizing endogenous SMN isoforms. Because SMNΔ7 is a relatively good SCF^{Slmb} substrate, overexpression of this isoform protects full-length SMN from degradation.

As mentioned above, experiments in an SMN-deficient chicken DT40 cell line showed that expression of SMNΔ7A, but not SMNΔ7S, rescued cellular proliferation (Cho and Dreyfuss, 2010). These results suggest that, when stable, SMNΔ7 is intrinsically functional. To examine SMNΔ7A functionality in a more disease-relevant cell type, control and SMA-induced pluripotent stem cell (iPSC) motor neuron cultures were transduced with lentiviral vectors expressing an mCherry control protein or SMNΔ7A (Figure 6B). At 4 wk postdifferentiation, no statistical difference was observed between control and SMA motor neurons; however, by 6 wk, SMA motor neuron numbers had decreased significantly to ~7% of the total cell population (Figure 6B). In contrast, expression of SMNΔ7A maintained motor neuron numbers to approximately the same level as the controls and nearly twofold greater than untreated cells (Figure 6B). Thus expression of SMNΔ7A improves survival of human iPSCs when differentiated into motor neuron lineages.

SMNΔ7A is a protective modifier of intermediate SMA mouse phenotypes

To examine the importance of the Slmb degron in a mammalian organismal system, two previously developed SMA mouse models were utilized. As mentioned above, the "Delta7" mouse (*Smn*$^{-/-}$*;SMN2;SMN*Δ*7*) is a model of severe SMA (Le *et al.*, 2005), and affected pups usually die between P10 and P18 (avg. = P15). The "2B/–" mouse (*Smn*$^{2B/-}$) is a model of intermediate SMA (Bowerman *et al.*, 2012; Rindt *et al.*, 2015) and these animals survive much longer, typically between P25 and P45 (avg. = P32). Adeno-associated virus serotype 9 (AAV9) was selected to deliver the SMN cDNA isoforms to these SMA mice, as this vector has previously been shown to enter and express in SMA-relevant tissues and can dramatically rescue the SMA phenotype when expressing the wild-type SMN cDNA (Foust *et al.*, 2010; Passini *et al.*, 2010; Valori *et al.*, 2010; Dominguez *et al.*, 2011; Glascock *et al.*, 2012).

Delivery of AAV9-SMNΔ7A at P1 significantly extended survival in the intermediate 2B/– animals, resulting in 100% of the treated pups living beyond 100 d, similar to the results obtained with the full-length AAV9-SMN construct (Figure 7A). In contrast, untreated 2B/– animals lived, on average, only 30 d. Mice treated with AAV9-SMNΔ7S survived an average of 45 d (Figure 7A). Mice treated with AAV9-SMNΔ7D, a phosphomimetic of the wild-type serine 270 residue, have an average life span that is equivalent or slightly shorter than that of untreated 2B/– mice (Figure 7A). These results not only highlight the specificity of the S270A mutation in conferring efficacy to SMNΔ7 but also illustrate that AAV9-mediated delivery of protein alone does not improve the phenotype.

We also analyzed the effects of SMNΔ7A expression in the severe Delta7 mouse model (Le *et al.*, 2005). Treatment with AAV9-SMNΔ7A had only a very modest effect on Delta7 mice, as none of the animals (treated or untreated) survived weaning (Supplemental Figure S4). These findings are similar to the results in *Drosophila*. Transgenic expression of SMNΔ7A in the *Smn* null background is not sufficient to rescue larval lethality (Supplemental Figure S3). Thus expression of SMNΔ7A provides a clear protective benefit to the viability of intermediate mice but not to severe SMA models.

Consistent with the life-span data, AAV9-SMNΔ7A treated 2B/– mice gained significantly more weight than either untreated or AAV-SMNΔ7S-treated animals, nearly achieving the same weight as pups treated with full-length AAV-SMN (Figure 7B). Treatment with full-length SMN cDNA resulted in animals that were clearly stronger and more mobile, consistent with the weight data (Figure 7C). Although they did not perform as well as mice treated with full-length SMN cDNA, the SMNΔ7A-treated animals retained strength and gross motor function at late time points (e.g., P100), as measured by their ability to splay their legs and maintain a hanging position using a modified tube test, (Figure 7C). Animals treated with AAV9-SMNΔ7D and -SMNΔ7S did not survive long enough for testing.

SCF^{Slmb} primarily targets unstable SMN monomers

As indicated in Figure 8, our findings suggest a model whereby SMN and SMNΔ7 degradation is in part mediated by SCF^{Slmb}, a multicomponent E3 ubiquitin ligase composed of Slmb, SkpA, Cul1, and Roc1 (Jiang and Struhl, 1998, Patton *et al.*, 1998a,b; Zheng *et al.*, 2002). Our work demonstrates that B-TrCP/Slmb binds directly to SMN (Figure 2) and is one of a growing number of E3 ligases in the cell that can target SMN protein (Kwon *et al.*, 2013; Han *et al.*, 2016). SMN monomers, such as those created in SMNΔ7, are the primary targets for degradation. As shown in the model, partially active SMN•SMNΔ7 dimers and active SMN oligomers are also substrates but to a lesser extent.

DISCUSSION

Factors that recognize the putative SMNΔ7-specific degron have not been identified, and the molecular mechanisms governing proteasomal access to SMN and SMNΔ7 remain unclear. In this study, we

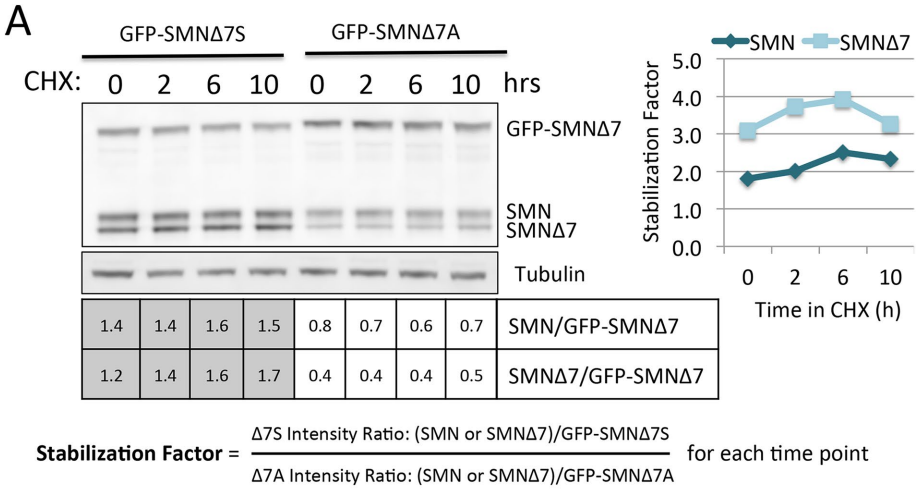

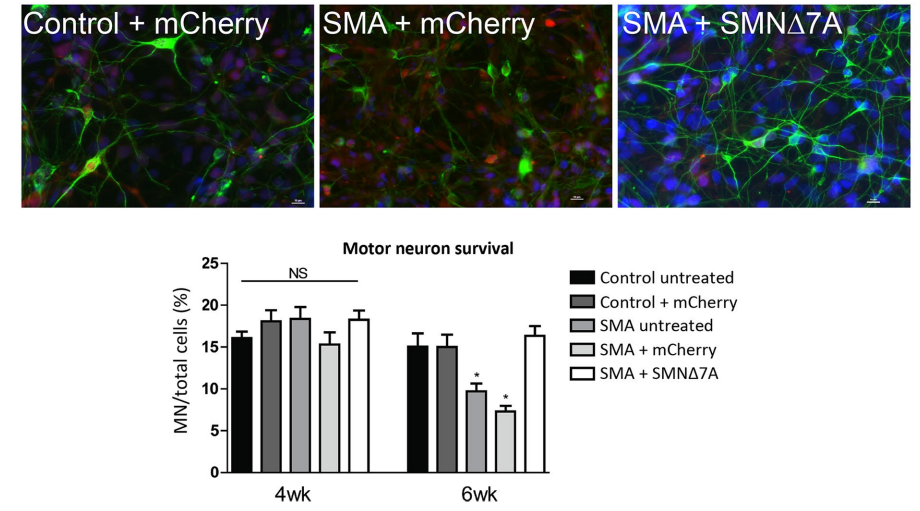

FIGURE 6: Stabilization of endogenous SMN and SMNΔ7 in cultured human cells. (A) HEK 293T cells were transfected with equivalent amounts of GFP-SMNΔ7A or -SMNΔ7S. The following day, cells were harvested after treatment with cycloheximide (CHX) for zero to 10 h. Western blotting with anti-SMN showed that SMNΔ7S stabilizes endogenous SMN and SMNΔ7 to a greater extent than SMNΔ7A. By comparing band intensities within a given lane, we generated average intensity ratios for each time point using replicate blots. We then calculated a "stabilization factor" by taking a ratio of these two ratios. The protective benefit of overexpressing Δ7S vs. Δ7A at $t = 0$ h was roughly 3.0× for endogenous SMNΔ7 and 1.75× for full-length SMN. (B) SMNΔ7A (S270A) expression protects SMA iPSC-derived motor neurons. Control motor neurons were left untreated or transduced with a lentiviral vector expressing an mCherry control. SMA motor neurons were left untreated or transduced with a lentiviral vector expressing an mCherry control or a lentiviral vector expressing SMNΔ7A (S270A). At 4 wk of differentiation, there was no difference in motor neuron survival between control and SMA iPSC motor neuron cultures in any of the treatment groups. However, at 6 wk, SMI-32-positive motor neurons showed selective loss in SMA iPSC motor neuron cultures in the untreated and lenti-mCherry groups compared with control iPSC motor neuron cultures. In contrast, lenti-SMNΔ7A expression fully protects SMA iPSC-derived motor neurons. Representative images of control and SMA iPSC-derived motor neurons labeled with SMI-32 (green) and mCherry (red). Nuclei are stained with 4′,6-diamidino-2-phenylindole (DAPI) and shown in blue. *$p < 0.05$ by ANOVA. NS = not significant. $n = 3$

isolated factors that copurifiy with SMN from *Drosophila* embryos that exclusively express Flag-SMN. This approach reduces potential bias towards SMN partner proteins that may be more abundant in a given tissue or cell line (Charroux *et al.*, 1999; Meister *et al.*, 2001; Pellizzoni *et al.*, 2002; Kroiss *et al.*, 2008; Trinkle-Mulcahy *et al.*, 2008; Guruharsha *et al.*, 2011). Here we identify the SCF^{Slmb} E3 ubiquitin ligase complex as a novel SMN binding partner whose interaction is conserved in human. Depletion of Slmb or B-TrCP by RNAi resulted in an increase in steady-state SMN levels in *Drosophila* and human cells, respectively. We also showed that ectopic expression of SMNΔ7^{S270A}, but not SMNΔ7 or SMNΔ7^{S270D}, a phosphomimetic, is a protective modifier of SMA phenotypes in animal models and human iPSC cultures.

The SCF^{Slmb} degron is exposed by *SMN2* exon skipping

A previous study posited that a phosphodegron was specifically created by exon 7 skipping and that this event represented a key aspect of the SMA disease mechanism (Cho and Dreyfuss, 2010). Our identification of a putative Slmb binding site located in the C-terminal self-oligomerization domain of *Drosophila* and human SMN has allowed us to explore the molecular details of this hypothesis. The mutation of a conserved serine within the Slmb degron not only disrupted the interaction between SMN and Slmb but also stabilized full-length SMN and SMNΔ7. Notably, the degron mutation has a greater effect on SMN levels (both full-length and Δ7) when made in the context of a protein that does not efficiently self-oligomerize. These and other findings strongly suggest that the Slmb degron is uncovered when SMN is monomeric, whereas it is less accessible when SMN forms higher-order multimers. On the basis of these results, we conclude that *SMN2* exon skipping does not *create* a potent protein degradation signal; rather, it *exposes* an existing one.

SMN targeting by multiple E2 and E3 systems

SMN degradation via the UPS is well established (Chang *et al.*, 2004; Burnett *et al.*, 2009; Kwon *et al.*, 2011). Using candidate approaches, investigators have studied other E3 ligases that have been reported to target SMN for degradation in cultured human cells (Hsu *et al.*, 2010; Kwon *et al.*, 2013; Han *et al.*, 2016). Given our findings, it is therefore likely that SMN is targeted by multiple E3 ubiquitin ligases, as this regulatory paradigm has been demonstrated for a number of proteins (e.g., p53; Jain and Barton, 2010). Targeting of a single protein by multiple E3 ligases is thought to provide regulatory specificity by expressing the appropriate degradation complexes only within certain tissues, subcellular compartments, or developmental time frames. Moreover, ubiquitylation does not always result in immediate destruction of the target; differential use of ubiquitin lysine linkages or chain length can alter a protein's fate (Mukhopadhyay and Riezman, 2007; Ikeda and Dikic, 2008; Liu and Walters, 2010).

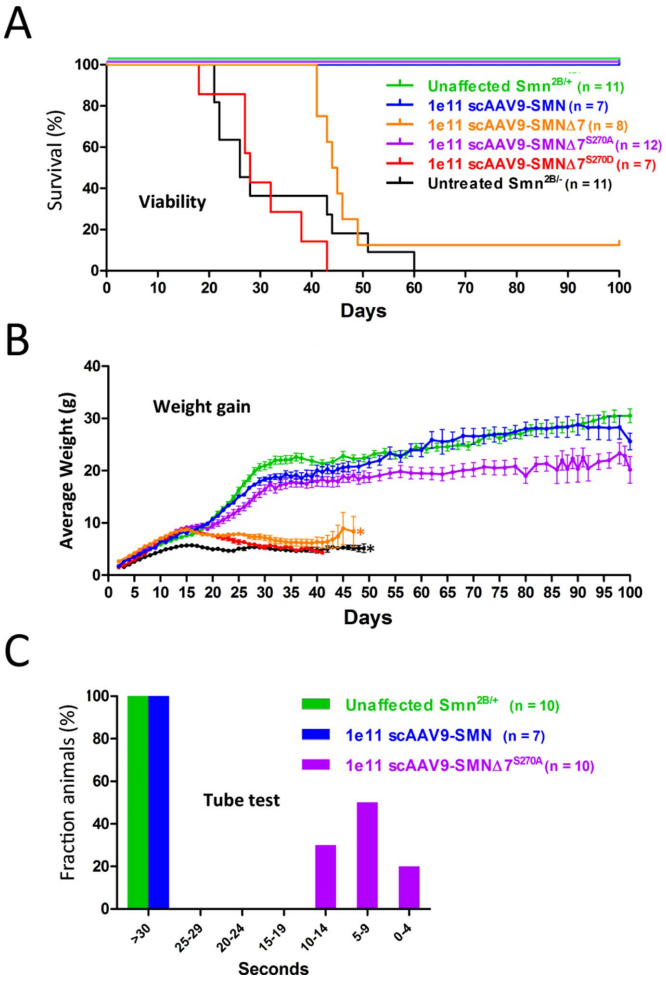

FIGURE 7: SMNΔ7A is a protective modifier of intermediate SMA phenotypes in mice. (A) Mouse genotypes include control unaffected *Smn*$^{2B/+}$ mice, which have a wild-type *Smn* allele, *Smn*$^{2B/-}$ (2B/–) mice treated with scAAV9 expressing different versions of SMN, and untreated 2B/– mice, which are an intermediate mouse model of SMA. 1e11 denotes the viral dose. scAAV9-SMN expresses full-length SMN, scAAV9-SMNΔ7 expresses truncated SMN, scAAV9-SMNΔ7^{S270A} expresses truncated SMN with the S-to-A change in the degron, and scAAV9-SMNΔ7^{S270D} expresses truncated SMN with a phosphomimic in the degron. Delivery of AAV9-SMNΔ7A at P1 significantly extended survival in the intermediate 2B/– animals, resulting in 100% of the treated pups living beyond 100 d, similar to the results obtained with the full-length AAV9-SMN construct. Untreated 2B/– animals lived, on average, only 30 d. Mice treated with AAV9-SMNΔ7S survived an average of 45 d. Mice treated with AAV9 expressing SMNΔ7D had an average life span equivalent or slightly worse than that of untreated 2B/– mice. (B) Average weight (measured over time) of the animals used in panel A. AAV9-SMNΔ7A treated mice also gained significantly more weight than either untreated or AAV-SMNΔ7S-treated animals, nearly achieving the same weight as 2B/– pups treated with full-length SMN cDNA. (C) Mouse genotypes include control unaffected *Smn*$^{2B/+}$ mice, which carry a wild-type *Smn* allele, and 2B/– mice treated with scAAV9 expressing different versions of SMN. scAAV9-SMN expresses full-length SMN and scAAV9-SMNΔ7^{S270A} expresses truncated SMN with the S-to-A change in the degron. AAV-SMNΔ7A-treated animals retained their improved strength and gross motor functions at late time points (P100), as measured by their ability to splay their legs and maintain a hanging position using a modified tube test.

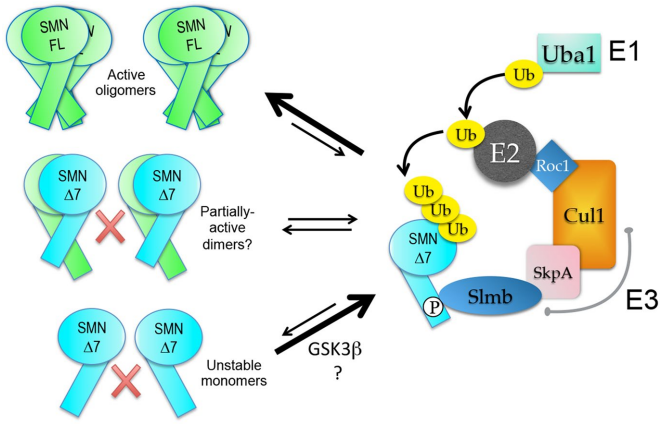

FIGURE 8: Proposed model of SMN as a substrate of SCF^{Slmb} E3 ubiquitin ligase. Unstable SMN monomers, such as those created in SMNΔ7, are the primary substrates for degradation. Active oligomers of full-length SMN (SMN-FL) and partially active SMN-FL•SMNΔ7 dimers (Praveen *et al.*, 2014; Gupta *et al.*, 2015) would be targeted to a lesser extent. SCF^{Slmb} is a multicomponent E3 ubiquitin ligase composed of Slmb, SkpA, Cul1, and Roc1 (see the text for details). This E3 ligase complex functions together with E1 and E2 proteins in the ubiquitin proteasome system (UPS) to tag proteins for degradation by linkage to ubiquitin (Ub). Phosphorylation (P) by GSK3β and/or another kinase (see the text) is predicted to trigger ubiquitylation.

Avenues of future exploration include determination of the E2 proteins that partner with SCF^{Slmb} as well as the types of ubiquitin lysine chain linkages they add to SMN. These two questions are interconnected, as ubiquitin linkage specificity is determined by the E2 (Ye and Rape, 2009). Lysine 48 (K48) linked chains typically result in degradation of the targeted protein by the 26S proteasome, whereas lysine 63 (K63) linkage is more commonly associated with lysosomal degradation and nonproteolytic functions such as endocytosis (Tan *et al.*, 2008; Kirkin *et al.*, 2009; Lim and Lim, 2011). Interestingly, recent work has implicated defects in endocytosis in SMA (Custer and Androphy, 2014; Dimitriadi *et al.*, 2016; Hosseinibarkooie *et al.*, 2016). It remains to be determined how the ubiquitylation status of SMN might intersect with endocytic functions.

Does SMN function as a signaling hub?

In the Flag-SMN pull down, we identified three E2 proteins as potential SMN interacting partners (Figure 1C). Among them, Bendless (Ben) is particularly interesting. Ben physically interacts with TRAF6, an E3 ligase that functions together with Ube2N/Ubc13/Ben in human cells (Kim and Choi, 2017). TRAF6 is an activator of NF-kB signaling, and its interaction with SMN is thought to inhibit this activity (Kim and Choi, 2017). Notably, Ube2N/Ben heterodimerizes with Uev1a to form K63 ubiquitin linkages on target proteins (Ye and Rape, 2009; van Wijk and Timmers, 2010; Komander and Rape, 2012; Marblestone *et al.*, 2013; Zhang *et al.*, 2013). Furthermore, Ben-Uev1a is involved in upstream activation of both JNK (Jun Nuclear Kinase) and IMD (Immune Deficiency) signaling in *Drosophila* (Zhou *et al.*, 2005; Paquette *et al.*, 2010). Previously, we and others have shown that JNK signaling is dysregulated in animal models of SMA (Garcia *et al.*, 2013, 2016; Genabai *et al.*, 2015; Ahmad *et al.*, 2016). Moreover, mutations in all three components of SCF^{Slmb} lead to constitutive expression of antimicrobial peptides, which are also downstream of the IMD pathway (Khush *et al.*, 2002). Together, these findings suggest the interesting possibility of SMN

functioning as a signaling hub that links the UPS to the JNK and IMD pathways, all of which have been shown to be disrupted in SMA.

Phosphorylation of the Slmb degron within SMN

As Slmb is known to recognize phospho-degrons, one of the first questions raised by our study concerns the identity of the kinase(s) responsible for phosphorylating the degron in SMN. A prime candidate is GSK3β (Figure 8), as this kinase recognizes a motif (SxxxS/T; Liu *et al.,* 2007; Lee *et al.,* 2013) that includes the degron and extends N-terminally (^{262}SxxxSxxxSxxxT^{274}, numbering as per human SMN). In support of this hypothesis, we identified the *Drosophila* GSK3β orthologue, Shaggy (Sgg), in our SMN pull downs (Figure 1C). Moreover, GSK3β inhibitors as well as siRNA-mediated knockdown of GSK3β were shown to increase SMN levels, primarily by stabilizing the protein (Makhortova *et al.,* 2011; Chen *et al.,* 2012). Finally, GSK3β is also responsible for phosphorylation of a degron in β-catenin, a well-characterized SCF^{Slmb} substrate (Liu *et al.,* 2002). SMA mice have low levels of UBA1 (E1), ultimately leading to accumulation of β-catenin (Wishart *et al.,* 2014). Pharmacological inhibition of β-catenin improved neuromuscular pathology in *Drosophila*, zebrafish, and mouse SMA models. β-Catenin had previously been shown to regulate motor neuron differentiation and stability by affecting synaptic structure and function (Murase *et al.,* 2002; Li *et al.,* 2008; Ojeda *et al.,* 2011). β-Catenin also regulates motor neuron differentiation by retrograde signaling from skeletal muscle (Li *et al.,* 2008). The connections of UBA1 and multiple SCF^{Slmb} substrates to motor neuron health thus places the UPS at the center of SMA research interest.

Concluding remarks

In summary, this study identifies conserved factors that regulate SMN stability. To our knowledge, this work represents the first time that SMN complexes have been purified in the context of an intact developing organism. Using this approach, we have demonstrated that the SCF^{Slmb} E3 ligase complex interacts with a degron embedded within the self-oligomerization domain of SMN. Our findings establish plausible connections to disease-relevant cellular processes and signaling pathways. Further, they elucidate a model (Figure 8) whereby accessibility of the SMN phosphodegron is regulated by self-multimerization, providing an elegant mechanism for balancing functional activity with degradation.

MATERIALS AND METHODS

Fly stocks and transgenes

Oregon-R was used as the wild-type control. The Smn^{X7} microdeletion allele (Chang *et al.,* 2008) was a gift from S. Artavanis-Tsakonis (Harvard University, Cambridge, MA). This deficiency removes the promoter and the entire SMN coding region, leaving only the final 44 base pairs of the 3′ untranslated region (UTR). All stocks were cultured on molasses and agar at room temperature (24 ± 1°C) in half-pint bottles. The Smn transgenic constructs were injected into embryos by BestGene (Chino Hills, CA) as described in Praveen *et al.,* 2014. In short, a ~3 kb fragment containing the entire *Smn* coding region was cloned from the *Drosophila* genome into the pAttB vector (Bischof *et al.,* 2007). A 3X FLAG tag was inserted immediately downstream of the start codon of dSMN. Point mutations were introduced into this construct using Q5 (NEB) site-directed mutagenesis according to manufacturer's instructions. The basal Smn construct used, vSmn, contained three single-amino-acid changes, and the addition of the MGLR motif to make fruit fly Smn more similar to the evolutionarily conserved vertebrate Smn. Subsequently generated constructs used vSmn as a template and consist of the amino acid changes detailed in Figure 4. Y203C, G206S, and G210V were previously published in Praveen *et al.,* 2014.

Drosophila embryo protein lysate and mass spectrometry

Drosophila embryos (0–12 h) were collected from Oregon-R control and Flag-SMN flies, dechorionated, flash frozen, and stored at –80°C. Embryos (approximately 1 g) were then homogenized on ice with a Potter tissue grinder in 5 ml of lysis buffer containing 100 mM potassium acetate, 30 mM HEPES–KOH at pH 7.4, 2 mM magnesium acetate, 5 mM dithiothreitol (DTT), and protease inhibitor cocktail. Lysates were centrifuged twice at 20,000 rpm for 20 min at 4°C and dialyzed for 5 h at 4°C in Buffer D (HEPES 20 mM, pH 7.9, 100 mM KCl, 2.5 mM $MgCl_2$, 20% glycerol, 0.5 mM DTT, phenylmethylsulfonyl fluoride [PMSF] 0.2 mM). Lysates were clarified again by centrifugation at 20,000 rpm for 20 min at 4°C. Lysates were flash frozen using liquid nitrogen and stored at –80°C before use. Lysates were then thawed on ice, centrifuged at 20,000 rpm for 20 min at 4°C and incubated with rotation with 100 µl of EZview Red Anti-FLAG M2 affinity gel (Sigma) for 2 h at 4°C. Beads were washed a total of six times using buffer with KCl concentrations ranging from 100 to 250 mM with rotation for 1 min at 4°C in between each wash. Finally, Flag proteins were eluted 3 consecutive times with one bed volume of elution buffer (Tris 20 mM, pH 8, 100 mM KCl, 10% glycerol, 0.5 mM DTT, PMSF 0.2 mM) containing 250 µg/ml 3XFLAG peptide (sigma). The entire eluate was used for mass spectrometry analysis on an Orbitrap Velos instrument, fitted with a Thermo Easy-spray 50-cm column.

Tissue culture and transfections

S2 cell lines were obtained from the Drosophila Genome Resource Center (Bloomington, IL). S2 cells were maintained in SF900 serum-free medium (SFM) (Life Technologies) supplemented with 1% penicillin/streptomycin and filter sterilized. Cells were removed from the flask using a cell scraper and passaged to maintain a density of ~10^6–10^7 cells/ml. S2 cells were transferred to filter sterilized SF900 SFM (Life Technologies) without antibiotics prior to transfection with Cellfectin II (Invitrogen). Transfections were performed according to Cellfectin II protocol in a final volume of 4 ml in a T-25 flask containing 10^7 cells that were plated 1 h before transfection. The total amount of DNA used in transfections was 2.5 µg. Human embryonic kidney HEK-293T and HeLa cells were maintained at 37°C with 5% CO_2 in DMEM (Life Technologies) supplemented with 10% fetal bovine serum (FBS) and 1% penicillin/streptomycin (Life Technologies). Cells (1×10^6–2×10^6) were plated in T-25 flasks and transiently transfected with 1–2 µg of plasmid DNA per flask using Lipofectamine (Invitrogen) or FuGENE HD transfection reagent (Roche Applied Science, Indianapolis, IN) according to the manufacturer's protocol. Cells were harvested 24–72 h posttransfection.

For siRNA transections, HeLa cells were plated subconfluently in T-25 flasks and transfected with 10 nm of siRNA (gift from Mike Emanuele lab) and 17 µl Lipofectamine RNAi MAX (Invitrogen) in 5 ml total media according to manufacturer's instructions. After 48 h of transfection, cells were harvested. For RNAi in S2 cells using dsRNA, 10^7 cells were plated in each well of a six-well plate in 1 ml of media. Cells were treated approximately every 24 h with 10 µg/ml dsRNA targeted against Slmb, Oskar, or Gaussia Luciferaese (as controls) as described in Rogers and Rogers, 2008.

In vitro binding assay

GST and GST-SMN were purified from *Escherichia coli*. In brief, cells transformed with BL21*GST-SMN were grown at 37°C overnight and then induced using 1 mM isopropyl-β-D-thiogalactopyranoside (IPTG). Recombinant protein was extracted and purified using

glutathione sepharose 4B beads. GST-B-TrCP1 was purchased from Novus Biologicals (cat# H00008945). SMN•Gem2 complexes were coexpressed in *E. coli* using SMNΔ5 and Gemin2(12–280) constructs, as described in Gupta et al. (2015). Glutathione sepharose 4B beads were washed 3× with phosphate-buffered saline (PBS). GST alone, GST-SMN, or GST-B-TrCP1 were attached to beads during 4-h-overnight incubation at 4°C in PBS with rotation. Beads were then washed 3× with modified radioimmunoprecipitation assay (RIPA) buffer (50 mM Tris-HCl, pH 7.5, 250 mM NaCl, 1 mM EDTA, 1% NP-40). Beads (20 µl) with ~2 µg attached GST-tagged protein (as determined by Coomassie stain with bovine serum albumin [BSA] standard) were added to 200 µl modified RIPA buffer with 100 µg/ml BSA block. SMN•Gem2 (2 µg) was added, and the mixture was rotated end over end at 4°C overnight. Beads were then washed 3× with modified RIPA buffer, and 10 µl SDS loading buffer was added followed by boiling for 5 min.

In vivo ubiquitylation assay

The in vivo ubiquitylation assay was performed as described previously (Choudhury *et al.*, 2016). Briefly, HEK-293T cells were transfected as indicated in 10-cm dishes using Lipofectamine2000 (Thermo Fisher Scientific). The day after, cells were treated with 20 µM of MG132 for 4 h and then harvested in PBS. Of the cell suspension, 80% was lysed in 6 M guanidine-HCl–containing buffer and used to pull down His-Ubiquitinated proteins on Ni2+-NTA beads, while the remaining 20% was used to prepare inputs. Ni2+ pull-down eluates and inputs were separated through SDS–PAGE and analyzed by Western blot.

Cycloheximide treatment

Following RNAi treatment, S2 cells were pooled, centrifuged, and resuspended in fresh media. One-third of these cells were frozen and taken as the 0 h time point. The remainders of the cells were replated in six-well plates. Cycloheximide (CHX; 100 µg/ml) was added to each sample, and cells were harvested at 2 and 6 h following treatment.

Immunoprecipitation

Clarified cell lysates were precleared with immunoglobulin G agarose beads for 1 h at 4°C and again precleared overnight at 4°C. The precleared lysates were then incubated with anti-FLAG antibody cross-linked to agarose beads (EZview Red Anti-FLAG M2 affinity gel, Sigma) for 2 h at 4°C with rotation. The beads were washed with lysis buffer or modified lysis buffer six times and boiled in SDS gel-loading buffer. Eluted proteins were run on an SDS–PAGE for Western blotting.

Antibodies and Western blotting

Larval and adult lysates were prepared by crushing the animals in lysis buffer (50 mM Tris-HCl, pH 7.5, 150 mM NaCl, 1 mM EDTA, 1% NP-40) with 1× (adults) or 10× (larvae) protease inhibitor cocktail (Invitrogen) and clearing the lysate by centrifugation at 13,000 rpm for 10 min at 4°C. S2 cell lysates were prepared by suspending cells in lysis buffer (50 mM Tris-HCl, pH 7.5, 150 mM NaCl, 1 mM EDTA, 1% NP-40) with 10% glycerol and 1× protease inhibitor cocktail (Invitrogen) and disrupting cell membranes by pulling the suspension through a 25-gauge needle (Becton Dickinson). The lysate was then cleared by centrifugation at 13,000 rpm for 10 min at 4°C. Human cells (293T and HeLa) were first gently washed in ice-cold 1× PBS and then collected in ice-cold 1× PBS by scraping. Cells were pelleted by spinning at 1000 rpm for 5 min. The supernatant was removed, and cells were resuspended in ice-cold lysis buffer (50 mM Tris-HCl, pH 7.5, 150 mM NaCl, 1 mM EDTA, 1% NP-40) and allowed to lyse on ice for 30 min. After lysing, the lysate was cleared by centrifuging the cells for 10 min at 13,000 rpm at 4°C. Western blotting on lysates was performed using standard protocols. Rabbit anti-dSMN serum was generated by injecting rabbits with purified full-length dSMN protein (Pacific Immunology Corp.) and was subsequently affinity purified. For Western blotting, dilutions of 1 in 2500 for the affinity purified anti-dSMN, 1 in 20,000 (fly) or 1 in 5000 (human) for anti–α-tubulin (Sigma), 1 in 10,000 for monoclonal anti-Flag (Sigma), 1 in 1000 for anti-Slmb (gift from Greg Rogers, University of Arizona), 1 in 2500 for anti-human SMN (BD Biosciences), 1 in 1000 for anti–B-TrCP (gift from Ben Major, University of North Carolina, Chapel Hill), 1 in 10,000 for polyclonal anti-Myc (Santa Cruz), and 1 in 2000 for anti-GST (Abcam) were used.

Larval locomotion

Smn control and mutant larvae (73–77 h post–egg laying) were placed on a 1.5% agarose molasses tray five at a time. The tray was then placed in a box with a camera, and the larvae were recorded moving freely for 60 s. Each set of larvae was recorded three times, and one video was chosen for analysis based on video quality. The videos were then converted to AVI files and analyzed using the wrMTrck plug-in of the Fiji software. The "Body Lengths per Second" was calculated in wrMTrck by dividing the track length by half the perimeter and time (seconds). *p* Values were generated using a multiple comparison analysis of variance (ANOVA).

SMA mouse models

Two previously developed SMA mouse models were utilized. The "Delta7" mouse (*Smn*$^{-/-}$;*SMN2*;*SMNΔ7*) is a model of severe SMA (Le *et al.*, 2005). The "2B/–" mouse (*Smn*$^{2B/-}$) is a model of intermediate SMA (Bowerman *et al.*, 2012; Rindt *et al.*, 2015). Adeno-associated virus serotype 9 (AAV9) delivered SMN cDNA isoforms to these SMA mice, as previously described (Foust *et al.*, 2010; Passini *et al.*, 2010; Valori *et al.*, 2010; Dominguez *et al.*, 2011; Glascock *et al.*, 2012). Gross motor function was measured using a modified tube test which tests the ability of mice to splay their legs and maintain a hanging position.

Human iPSC cell culture

Human iPSCs from two independent unaffected control and two SMA patient lines were grown as pluripotent colonies on Matrigel substrate (Corning) in Nutristem medium (Stemgent). Colonies were then lifted using 1 mg/ml Dispase (Life Technologies) and maintained as floating spheres of neural progenitor cells in the neural progenitor growth medium Stemline (Sigma) supplemented with 100 ng/ml human basic fibroblast growth factor (FGF-2; Miltenyi), 100 ng/ml epidermal growth factor (EGF; Miltenyi), and 5 µg/ml heparin (Sigma-Aldrich) in ultra-low attachment flasks. Aggregates were passaged using a manual chopping technique as previously described (Svendsen *et al.*, 1998; Ebert *et al.*, 2013). To induce motor neuron differentiation, neural progenitor cells were cultured in neural induction medium (1:1 DMEM/F12 [Life Technologies], 1× N2 Supplement [Life Technologies], 5 µg/ml Heparin [Sigma], 1× Non-Essential Amino Acids [Life Technologies], and 1× Antibiotic-Antimycotic [Life Technologies]) plus 0.1 µM all-trans retinoic acid (RA) for 2 wk; 1 µM Purmorphamine (PMN; Stemgent) was added during the second week. Spheres were then dissociated with TrypLE Express (Life Technologies) and plated onto Matrigel-coated 12-mm coverslips in neural induction medium (NIM) plus 1 µM RA, 1 µM PMN, 1× B27 Supplement (Life Technologies), 200 ng/ml ascorbic acid (Sigma), 1 µM cAMP (Sigma), 10 ng/ml brain-derived

neurotrophic factor (BDNF; Peprotech), and 10 ng/ml glial cell line–derived neurotrophic factor (GDNF; Peprotech). One week postplating, cells were infected with lentiviral vectors (multiplicity of infection = 5) expressing mCherry alone or SMN S270A-IRES-mCherry. Transgenes in both viruses were under the control of the EF1α promoter. Uninfected cells served as controls. Cells were analyzed at 1 and 3 wk postinfection, which was 4 and 6 wk of total differentiation (Ebert *et al.*, 2009; Sareen *et al.*, 2013).

Immunocytochemistry

Coverslips were fixed in 4% paraformaldehyde (Electron Microscopy Sciences) for 20 min at room temperature and rinsed with PBS. Cells were blocked with 5% normal donkey serum (Millipore) and permeabilized in 0.2% Triton X-100 (Sigma) for 30 min at room temperature. Cells were then incubated in primary antibody solution for 1 h, rinsed with PBS and incubated in secondary antibody solution for 1 h at room temperature. Finally, nuclei were labeled with Hoechst nuclear stain (Sigma) to label DNA and mounted onto glass slides using FluoroMount medium (SouthernBiotech). Primary antibodies used were mouse anti–SMI-32 (Covance SMI-32R; 1:1000) and rabbit anti-mCherry (ThermoFisher; 1:1000). Secondary antibodies used were donkey anti-rabbit Cy3 (Jackson Immunoresearch 711–165–152) and donkey anti-mouse AF488 (Invitrogen A21202).

Immunocytochemical analysis

Images were acquired from five random fields per coverslip using an inverted fluorescent microscope (Nikon) and NIS Elements software. Images were blinded and manually analyzed for antigen specificity with NIS Elements software.

ACKNOWLEDGMENTS

This work was supported by National Institute of General Medical Sciences R01-GM118636 (to A.G.M.). K.M.G. was supported by graduate research fellowship DGE-1144081 from the National Science Foundation. Work in the Wagner lab (D.B. and E.J.W.) was supported by the Welch Foundation (H1889). We also thank the Peifer, Major, and Rogers laboratories for reagents, advice, and expertise.

REFERENCES

Ackermann B, Kröber S, Torres-Benito L, Borgmann A, Peters M, Hosseini Barkooie SM, Tejero R, Jakubik M, Schreml J, Milbradt J, *et al.* (2013). Plastin 3 ameliorates spinal muscular atrophy via delayed axon pruning and improves neuromuscular junction functionality. Hum Mol Genet 22, 1328–1347.

Ahmad S, Bhatia K, Kannan A, Gangwani L (2016). Molecular mechanisms of neurodegeneration in spinal muscular atrophy. J Exp Neurosci 10, 39–49.

Bischof J, Maeda RK, Hediger M, Karch F, Basler K (2007). An optimized transgenesis system for Drosophila using germ-line-specific phiC31 integrases. Proc Natl Acad Sci USA 104, 3312–3317.

Bowerman M, Anderson CL, Beauvais A, Boyl PP, Witke W, Kothary R (2009). SMN, profilin IIa and plastin 3: A link between the deregulation of actin dynamics and SMA pathogenesis. Mol Cell Neurosci 42, 66–74.

Bowerman M, Murray LM, Beauvais A, Pinheiro B, Kothary R (2012). A critical smn threshold in mice dictates onset of an intermediate spinal muscular atrophy phenotype associated with a distinct neuromuscular junction pathology. Neuromuscul Disord 22, 263–276.

Burghes Arthur HM, Beattie Christine E (2009). Spinal muscular atrophy: why do low levels of survival motor neuron protein make motor neurons sick? Nat Rev Neurosci 10, 597–609.

Burnett BG, Muñoz E, Tandon A, Kwon DY, Sumner CJ, Fischbeck KH (2009). Regulation of SMN protein stability. Mol Cell Biol 29, 1107–1115.

Cauchi RJ, Sanchez-Pulido L, Liu J-L (2010). Drosophila SMN complex proteins Gemin2, Gemin3, and Gemin5 are components of U bodies. Exp Cell Res 316, 2354–2364.

Chan YB, Miguel-Aliaga I, Franks C, Thomas N, Trülzsch B, Sattelle DB, Davies KE, van den Heuvel M (2003). Neuromuscular defects in a Drosophila survival motor neuron gene mutant. Hum Mol Genet 12, 1367–1376.

Chang HCH, Dimlich DN, Yokokura T, Mukherjee A, Kankel MW, Sen A, Sridhar V, Fulga TA, Hart AC, Van Vactor D, *et al.* (2008). Modeling spinal muscular atrophy in Drosophila. PLoS One 3, e3209.

Chang HC, Hung WC, Chuang YJ, Jong YJ (2004). Degradation of survival motor neuron (SMN) protein is mediated via the ubiquitin/proteasome pathway. Neurochem Int 45, 1107–1112.

Charroux B, Pellizzoni L, Perkinson RA, Shevchenko A, Mann M, Dreyfuss G (1999). Gemin3: a novel DEAD box protein that interacts with SMN, the spinal muscular atrophy gene product, and is a component of gems. J Cell Biol 147, 1181–1193.

Chen PC, Gaisina IN, El-Khodor BF, Ramboz S, Makhortova NR, Rubin LL, Kozikowski AP (2012). Identification of a maleimide-based glycogen synthase kinase-3 (GSK-3) inhibitor, BIP-135, that prolongs the median survival time of Δ7 SMA KO mouse model of spinal muscular atrophy. ACS Chem Neurosci 3, 5–11.

Cho S, Dreyfuss G (2010). A degron created by SMN2 exon 7 skipping is a principal contributor to spinal muscular atrophy severity. Genes Dev 24, 438–442.

Choudhury R, Bonacci T, Arceci A, Decaprio JA, Burke DJ, Emanuele MJ, Choudhury R, Bonacci T, Arceci A, Lahiri D, *et al.* (2016). APC/C and SCF cyclin F constitute a reciprocal feedback circuit controlling S-phase entry. Cell Reports 16, 3359–3372.

Coovert DD, Le TT, McAndrew PE, Strasswimmer J, Crawford TO, Mendell JR, Coulson SE, Androphy EJ, Prior TW, Burghes AHM (1997). The survival motor neuron protein in spinal muscular atrophy. Hum Mol Genet 6, 1205–1214.

Crawford TO, Pardo CA (1996). The neurobiology of childhood spinal muscular atrophy. Neurobiol Dis 3, 97–110.

Custer SK, Androphy EJ (2014). Autophagy dysregulation in cell culture and animals models of spinal muscular atrophy. Mol Cell Neurosci 61, 133–140.

Dimitriadi M, Derdowski A, Kalloo G, Maginnis MS, Bliska B, Sorkaç A, Q Nguyen KC, Cook SJ, Poulogiannis G, Atwood WJ, *et al.* (2016). Decreased function of survival motor neuron protein impairs endocytic pathways. Proc Natl Acad Sci USA 4377–4386.

Dominguez E, Marais T, Chatauret N, Benkhelifa-Ziyyat S, Duque S, Ravassard P, Carcenac R, Astord S, de Moura AP, Voit T, *et al.* (2011). Intravenous scAAV9 delivery of a codon-optimized SMN1 sequence rescues SMA mice. Hum Mol Genet 20, 681–693.

Ebert AD, Yu J, Rose FF, Mattis VB, Lorson CL, Thomson JA, Svendsen CN (2009). Induced pluripotent stem cells from a spinal muscular atrophy patient. Nature 457, 277–280.

Ebert AD, Shelley BC, Hurley AM, Onorati M, Castiglioni V, Patitucci TN, Svendsen SP, Mattis VB, McGivern J V., Schwab AJ, *et al.* (2013). EZ spheres: A stable and expandable culture system for the generation of pre-rosette multipotent stem cells from human ESCs and iPSCs. Stem Cell Res 10, 417–427.

Fan L, Simard LR (2002). Survival motor neuron (SMN) protein: role in neurite outgrowth and neuromuscular maturation during neuronal differentiation and development. Hum Mol Genet 11, 1605–1614.

Fischer U, Liu Q, Dreyfuss G (1997). The SMN-SIP1 complex has an essential role in spliceosomal snRNP biogenesis. Cell 90, 1023–1029.

Foust KD, Wang X, McGovern VL, Braun L, Bevan AK, Haidet AM, Le TT, Morales PR, Rich MM, Burghes AHM, *et al.* (2010). Rescue of the spinal muscular atrophy phenotype in a mouse model by early postnatal delivery of SMN. Nat Biotechnol 28, 271–274.

Frescas D, Pagano M (2008). Deregulated proteolysis by the F-box proteins SKP2 and B-TrCP: tipping the scales of cancer. Nat Rev Cancer 8, 438–449.

Fuchs SY, Spiegelman VS, Kumar KGS (2004). The many faces of B-TrCP E3 ubiquitin ligases: reflections in the magic mirror of cancer. Oncogene 23, 2028–2036.

Garcia EL, Lu Z, Meers MP, Praveen K, Matera AG (2013). Developmental arrest of Drosophila survival motor neuron (Smn) mutants accounts for differences in expression of minor intron-containing genes. RNA 19, 1510–1516.

Garcia EL, Wen Y, Praveen K, Matera AG (2016). Transcriptomic comparison of Drosophila snRNP biogenesis mutants reveals mutant-specific changes in pre-mRNA processing: implications for spinal muscular atrophy. RNA 22, 1215–1227.

Gates J, Lam G, Ortiz J, Losson R, Thummel CS (2004). Rigor mortis encodes a novel nuclear receptor interacting protein required for ecdysone

signaling during Drosophila larval development. Development 131, 25–36.
Genabai NK, Ahmad S, Zhang Z, Jiang X, Gabaldon CA, Gangwani L (2015). Genetic inhibition of JNK3 ameliorates spinal muscular atrophy. Hum Mol Genet 24, 6986–7004.
Glascock JJ, Shababi M, Wetz MJ, Krogman MM, Lorson CL (2012). Direct central nervous system delivery provides enhanced protection following vector mediated gene replacement in a severe model of spinal muscular atrophy. Biochem Biophys Res Commun 417, 376–381.
Groen EJN, Gillingwater TH (2015). UBA1: at the crossroads of ubiquitin homeostasis and neurodegeneration. Trends Mol Med 21, 622–632.
Gupta K, Martin R, Sharp R, Sarachan KL, Ninan NS, Van Duyne GD (2015). Oligomeric properties of survival motor neuron.gemin2 complexes. J Biol Chem 290, 20185–20199.
Guruharsha KG, Rual J-F, Zhai B, Mintseris J, Vaidya P, Vaidya N, Beekman C, Wong C, Rhee DY, Cenaj O, *et al.* (2011). A protein complex network of Drosophila melanogaster. Cell 147, 690–703.
Han KJ, Foster D, Harhaj EW, Dzieciatkowska M, Hansen K, Liu CW (2016). Monoubiquitination of survival motor neuron regulates its cellular localization and Cajal body integrity. Hum Mol Genet 25, 1392–1405.
Hosseinibarkooie S, Peters M, Torres-Benito L, Rastetter RH, Hupperich K, Hoffmann A, Mendoza-Ferreira N, Kaczmarek A, Janzen E, Milbradt J, *et al.* (2016). The power of human protective modifiers: PLS3 and CORO1C unravel impaired endocytosis in spinal muscular atrophy and rescue SMA phenotype. Am J Hum Genet 99, 647–665.
Hsieh-Li HM, Chang JG, Jong YJ, Wu MH, Wang NM, Tsai CH, Li H (2000). A mouse model for spinal muscular atrophy. Nat Genet 24, 66–70.
Hsu SH, Lai MC, Er TK, Yang SN, Hung CH, Tsai HH, Lin YC, Chang JG, Lo YC, Jong YJ (2010). Ubiquitin carboxyl-terminal hydrolase L1 (UCHL1). regulates the level of SMN expression through ubiquitination in primary spinal muscular atrophy fibroblasts. Clin Chim Acta 411, 1920–1928.
Ikeda F, Dikic I (2008). Atypical ubiquitin chains: new molecular signals. EMBO Rep 9, 536–542.
Jain AK, Barton MC (2010). Making sense of ubiquitin ligases that regulate p53. Cancer Biol Ther 10, 665–672.
Jiang J, Struhl G (1998). Regulation of the Hedgehog and Wingless signalling pathways by the F-box/WD40-repeat protein Slimb. Nature 391, 493–496.
Jin J, Ang XL, Shirogane T, Wade Harper J (2005). Identification of substrates for F-box proteins. Methods Enzymol 399, 287–309.
Kariya S, Park GH, Maeno-Hikichi Y, Leykekhman O, Lutz C, Arkovitz MS, Landmesser LT, Monani UR (2008). Reduced SMN protein impairs maturation of the neuromuscular junctions in mouse models of spinal muscular atrophy. Hum Mol Genet 17, 2552–2569.
Khush RS, Cornwell WD, Uram JN, Lemaitre B (2002). A ubiquitin-proteasome pathway represses the Drosophila immune deficiency signaling cascade. Curr Biol 12, 1728–1737.
Kim EK, Choi E (2017). SMN1 functions as a novel inhibitor for TRAF6-mediated NF-κB signaling. BBA Mol Cell Res 1864, 760–770.
Kim TY, Siesser PF, Rossman KL, Goldfarb D, Mackinnon K, Yan F, Yi X, MacCoss MJ, Moon RT, Der CJ, *et al.* (2015). Substrate trapping proteomics reveals targets of the βTrCP2/FBXW11 ubiquitin ligase. Mol Cell Biol 35, 167–181.
Kirkin V, McEwan DG, Novak I, Dikic I (2009). A role for ubiquitin in selective autophagy. Mol Cell 34, 259–269.
Kolb SJ, Kissel JT (2015). Spinal muscular atrophy. Neurol Clin 33, 831–846.
Komander D, Rape M (2012). The ubiquitin code. Annu Rev Biochem 81, 203–229.
Kong L, Wang X, Choe DW, Polley M, Burnett BG, Bosch-Marce M, Griffin JW, Rich MM, Sumner CJ (2009). Impaired synaptic vesicle release and immaturity of neuromuscular junctions in spinal muscular atrophy mice. J Neurosci 29, 842–851.
Korhonen L, Lindholm D (2004). The ubiquitin proteasome system in synaptic and axonal degeneration: a new twist to an old cycle. J Cell Biol 165, 27–30.
Kroiss M, Schultz J, Wiesner J, Chari A, Sickmann A, Fischer U (2008). Evolution of an RNP assembly system: a minimal SMN complex facilitates formation of UsnRNPs in Drosophila melanogaster. Proc Natl Acad Sci USA 105, 10045–10050.
Kwon DY, Dimitriadi M, Terzic B, Cable C, Hart AC, Chitnis A, Fischbeck KH, Burnett BG (2013). The E3 ubiquitin ligase mind bomb 1 ubiquitinates and promotes the degradation of survival of motor neuron protein. Mol Biol Cell 24, 1863–1871.
Kwon DY, Motley WW, Fischbeck KH, Burnett BG (2011). Increasing expression and decreasing degradation of SMN ameliorate the spinal muscular atrophy phenotype in mice. Hum Mol Genet 20, 3667–3677.
Le TT, Pham LT, Butchbach MER, Zhang HL, Monani UR, Coovert DD, Gavrilina TO, Xing L, Bassell GJ, Burghes AHM (2005). SMNΔ7, the major product of the centromeric survival motor neuron (SMN2) gene, extends survival in mice with spinal muscular atrophy and associates with full-length SMN. Hum Mol Genet 14, 845–857.
Lee YC, Liao PC, Liou YC, Hsiao M, Huang CY, Lu PJ (2013). Glycogen synthase kinase 3 β activity is required for hBora/Aurora A-mediated mitotic entry. Cell Cycle 12, 953–960.
Lefebvre S, Bürglen L, Reboullet S, Clermont O, Burlet P, Viollet L, Benichou B, Cruaud C, Millasseau P, Zeviani M, *et al.* (1995). Identification and characterization of a spinal muscular atrophy-determining gene. Cell 80, 155–165.
Lefebvre S, Burlet P, Liu Q, Bertrandy S, Clermont O, Munnich A, Dreyfuss G, Melki J (1997). Correlation between severity and SMN protein level in spinal muscular atrophy. Nat Genet 16, 265–269.
Li DK, Tisdale S, Lotti F, Pellizzoni L (2014). SMN control of RNP assembly: from post-transcriptional gene regulation to motor neuron disease. Semin Cell Dev Biol 32, 22–29.
Li XM, Dong XP, Luo SW, Zhang B, Lee DH, Ting AKL, Neiswender H, Kim CH, Carpenter-Hyland E, Gao TM, *et al.* (2008). Retrograde regulation of motoneuron differentiation by muscle beta-catenin. Nat Neurosci 11, 262–268.
Lim KL, Lim GGY (2011). K63-linked ubiquitination and neurodegeneration. Neurobiol Dis 43, 9–16.
Liu C, Li Y, Semenov M, Han C, Baeg GH, Tan Y, Zhang Z, Lin X, He X (2002). Control of B-catenin phosphorylation/degradation by a dual-kinase mechanism. Cell 108, 837–847.
Liu F, Walters KJ (2010). Multitasking with ubiquitin through multivalent interactions. Trends Biochem Sci 35, 352–360.
Liu M, Tu X, Ferrari-Amorotti G, Calabretta B, Baserga R (2007). Downregulation of the upstream binding factor1 by glycogen synthase kinase3B in myeloid cells induced to differentiate. J Cell Biochem 100, 1154–1169.
Lorson CL, Rindt H, Shababi M (2010). Spinal muscular atrophy: mechanisms and therapeutic strategies. Hum Mol Genet 19, R111–R118.
Lorson CL, Androphy EJ (2000). An exonic enhancer is required for inclusion of an essential exon in the SMA-determining gene SMN. Hum Mol Genet 9, 259–265.
Lorson CL, Hahnen E, Androphy EJ, Wirth B (1999). A single nucleotide in the SMN gene regulates splicing and is responsible for spinal muscular atrophy. Proc Natl Acad Sci USA 96, 6307–6311.
Makhortova NR, Hayhurst M, Cerqueira A, Sinor-Anderson AD, Zhao WN, Heiser PW, Arvanites AC, Davidow LS, Waldon ZO, Steen JA, *et al.* (2011). A screen for regulators of survival of motor neuron protein levels. Nat Chem Biol 7, 544–552.
Marblestone JG, Butt S, McKelvey DM, Sterner DE, Mattern MR, Nicholson B, Eddins MJ (2013). Comprehensive ubiquitin E2 profiling of ten ubiquitin E3 ligases. Cell Biochem Biophys 67, 161–167.
Martin R, Gupta K, Ninan NS, Perry K, Van Duyne GD (2012). The survival motor neuron protein forms soluble glycine zipper oligomers. Structure 20, 1929–1939.
Matera AG, Wang Z (2014). A day in the life of the spliceosome. Nat Rev Mol Cell Biol 15, 108–121.
McWhorter ML, Monani UR, Burghes AHM, Beattie CE (2003). Knockdown of the survival motor neuron (Smn) protein in zebrafish causes defects in motor axon outgrowth and pathfinding. J Cell Biol 162, 919–931.
Meister G, Bühler D, Pillai R, Lottspeich F, Fischer U (2001). A multiprotein complex mediates the ATP-dependent assembly of spliceosomal U snRNPs. Nat Cell Biol 3, 1–8.
Monani UR, Sendtner M, Coovert DD, Parsons DW, Andreassi C, Le TT, Jablonka S, Schrank B, Rossoll W, Prior TW, *et al.* (2000). The human centromeric survival motor neuron gene (SMN2) rescues embryonic lethality in Smn(-/-) mice and results in a mouse with spinal muscular atrophy. Hum Mol Genet 9, 333–339.
Monani UR, Lorson CL, Parsons DW, Prior TW, Androphy EJ, Burghes AHM, McPherson JD (1999). A single nucleotide difference that alters splicing patterns distinguishes the SMA gene SMN1 from the copy gene SMN2. Hum Mol Genet 8, 1177–1183.
Mukhopadhyay D, Riezman H (2007). Proteasome-independent functions of ubiquitin in endocytosis and signaling. Science 315, 201–205.
Murase S, Mosser E, Schuman EM (2002). Depolarization drives β-catenin into neuronal spines promoting changes in synaptic structure and function. Neuron 35, 91–105.
Ning K, Drepper C, Valori CF, Ahsan M, Wyles M, Higginbottom A, Herrmann T, Shaw P, Azzouz M, Sendtner M (2010). PTEN depletion rescues axonal growth defect and improves survival in SMN-deficient motor neurons. Hum Mol Genet 19, 3159–3168.

Ogino S, Wilson RB (2004). Spinal muscular atrophy: molecular genetics and diagnostics. Expert Rev Mol Diagn 4, 15–29.
O'Hearn PJ, Garcia EL, Le TH, Hart AC, Matera AG, Beattie CE (2016). Non-mammalian animal models of SMA. In: Spinal Muscular Atrophy: Disease Mechanisms and Therapy, ed. C Sumner, S Paushkin, and C-P Ko, San Diego: Elsevier Academic Press, 221–239.
Ojeda L, Gao J, Hooten KG, Wang E, Thonhoff JR, Dunn TJ, Gao T, Wu P (2011). Critical role of PI3k/Akt/GSK3β in motoneuron specification from human neural stem cells in response to FGF2 and EGF. PLoS One 6, e23414.
Oprea GE, Kröber S, McWhorter ML, Rossoll W, Müller S, Krawczak M, Bassell GJ, Beattie CE, Wirth B (2008). Plastin 3 is a protective modifier of autosomal recessive spinal muscular atrophy. Science 320, 524–527.
Oskoui M, Darras B, De Vivo D (2016). Spinal muscular atrophy: 125 years later and on the verge of a cure. In: Spinal Muscular Atrophy: Disease Mechanisms and Therapy, ed. C Sumner, S Paushkin, and C-P Ko, San Diego: Elsevier Academic Press, 3–17.
Paquette N, Broemer M, Aggarwal K, Chen L, Husson M, Ertürk-Hasdemir D, Reichhart JM, Meier P, Silverman N (2010). Caspase-mediated cleavage, IAP binding, and ubiquitination: linking three mechanisms crucial for Drosophila NF-κB signaling. Mol Cell 37, 172–182.
Passini MA, Bu J, Roskelley EM, Richards AM, Sardi SP, O'Riordan CR, Klinger KW, Shihabuddin LS, Cheng SH (2010). CNS-targeted gene therapy improves survival and motor function in a mouse model of spinal muscular atrophy. J Clin Invest 120, 1253.
Patton EE, Willems AR, Sa D, Kuras L, Thomas D, Craig KL, Tyers M (1998a). Cdc53 is a scaffold protein for multiple Cdc34/Skp1/F-box protein complexes that regulate cell division and methionine biosynthesis in yeast. Genes Dev 12, 692–705.
Patton EE, Willems A, Tyers M (1998b). Combinatorial control in ubiquitin-dependent proteolysis: don't Skp the F-box hypothesis. Trends Genet 14, 236–243.
Pearn J (1980). Classification of spinal muscular atrophies. Lancet 315, 919–922.
Pellizzoni L, Yong J, Dreyfuss G (2002). Essential role for the SMN complex in the specificity of snRNP assembly. Science 298, 1775–1779.
Petroski MD (2008). The ubiquitin system, disease, and drug discovery. BMC Biochem 9(Suppl 1), S7.
Pillai RS, Grimmler M, Meister G, Will CL, Lührmann R, Fischer U, Schümperli D (2003). Unique Sm core structure of U7 snRNPs: assembly by a specialized SMN complex and the role of a new component, Lsm11, in histone RNA processing. Genes Dev 17, 2321–2333.
Praveen K, Wen Y, Gray KM, Noto JJ, Patlolla AR, Van Duyne GD, Matera AG (2014). SMA-causing missense mutations in survival motor neuron (Smn) display a wide range of phenotypes when modeled in Drosophila. PLoS Genet 10, e1004489.
Praveen K, Wen Y, Matera AG (2012). A Drosophila model of spinal muscular atrophy uncouples snRNP biogenesis functions of survival motor neuron from locomotion and viability defects. Cell Rep 1, 624–631.
Prior TW (2010). Spinal muscular atrophy: a time for screening. Curr Opin Pediatr 22, 696–702.
Rajendra TK, Gonsalvez GB, Walker MP, Shpargel KB, Salz HK, Matera AG (2007). A Drosophila melanogaster model of spinal muscular atrophy reveals a function for SMN in striated muscle. J Cell Biol 176, 831–841.
Ramser J, Ahearn ME, Lenski C, Yariz KO, Hellebrand H, von Rhein M, Clark RD, Schmutzler RK, Lichtner P, Hoffman EP, *et al.* (2008). Rare missense and synonymous variants in UBE1 are associated with X-linked infantile spinal muscular atrophy. Am J Hum Genet 82, 188–193.
Rindt H, Feng Z, Mazzasette C, Glascock JJ, Valdivia D, Pyles N, Crawford TO, Swoboda KJ, Patitucci TN, Ebert AD, *et al.* (2015). Astrocytes influence the severity of spinal muscular atrophy. Hum Mol Genet 24, 4094–4102.
Rogers SL, Rogers GC (2008). Culture of Drosophila S2 cells and their use for RNAi-mediated loss-of-function studies and immunofluorescence microscopy. Nat Protoc 3, 606–611.
Rossoll W, Jablonka S, Andreassi C, Kroning AK, Karle K, Monani UR, Sendtner M (2003). Smn, the spinal muscular atrophy-determining gene product, modulates axon growth and localization of beta-actin mRNA in growth cones of motoneurons. J Cell Biol 163, 801–812.
Sanchez G, Dury AY, Murray LM, Biondi O, Tadesse H, El Fatimy R, Kothary R, Charbonnier F, Khandjian EW (2013). A novel function for the survival motoneuron protein as a translational regulator. Hum Mol Genet 22, 668–684.
Sareen D, O'Rourke JG, Meera P, Muhammad AKMG, Grant S, Simpkinson M, Bell S, Carmona S, Ornelas L, Sahabian A, *et al.* (2013). Targeting RNA foci in iPSC-derived motor neurons from ALS patients with a C9ORF72 repeat expansion. Sci Transl Med 5, 1–13.
Schmutzler RK, Lichtner P, Hoffman EP (2008). Rare missense and synonymous variants in UBE1 are associated with X-linked infantile spinal muscular atrophy. Am J Hum Genet 82, 188–193.
Shafey D, Côté PD, Kothary R (2005). Hypomorphic Smn knockdown C2C12 myoblasts reveal intrinsic defects in myoblast fusion and myotube morphology. Exp Cell Res 311, 49–61.
Sharma A, Lambrechts A, Hao LT, Le TT, Sewry CA, Ampe C, Burghes AHM, Morris GE (2005). A role for complexes of survival of motor neurons (SMN) protein with gemins and profilin in neurite-like cytoplasmic extensions of cultured nerve cells. Exp Cell Res 309, 185–197.
Svendsen CN, Borg MG, Armstrong RJ, Rosser AE, Chandran S, Ostenfeld T, Caldwell MA (1998). A new method for the rapid and long term growth of human neural precursor cells. J Neurosci Methods 85, 141–152.
Tan JMM, Wong ESP, Kirkpatrick DS, Pletnikova O, Ko HS, Tay SP, Ho MWL, Troncoso J, Gygi SP, Lee MK, *et al.* (2008). Lysine 63-linked ubiquitination promotes the formation and autophagic clearance of protein inclusions associated with neurodegenerative diseases. Hum Mol Genet 17, 431–439.
Tiziano FD, Melki J, Simard LR (2013). Solving the puzzle of spinal muscular atrophy: what are the missing pieces? Am J Med Genet A 161A, 2836–2845.
Trinkle-Mulcahy L, Boulon S, Lam YW, Urcia R, Boisvert FM, Vandermoere F, Morrice NA, Swift S, Rothbauer U, Leonhardt H, *et al.* (2008). Identifying specific protein interaction partners using quantitative mass spectrometry and bead proteomes. J Cell Biol 183, 223–239.
Valori CF, Ning K, Wyles M, Mead RJ, Grierson AJ, Shaw PJ, Azzouz M (2010). Systemic delivery of scAAV9 expressing SMN prolongs survival in a model of spinal muscular atrophy. Sci Transl Med 2, 35–42.
van Wijk SJL, Timmers HTM (2010). The family of ubiquitin-conjugating enzymes (E2s): deciding between life and death of proteins. FASEB J 24, 981–993.
Voigt T, Meyer K, Baum O, Schümperli D (2010). Ultrastructural changes in diaphragm neuromuscular junctions in a severe mouse model for spinal muscular atrophy and their prevention by bifunctional U7 snRNA correcting SMN2 splicing. Neuromuscul Disord 20, 744–752.
Walker MP, Rajendra TK, Saieva L, Fuentes JL, Pellizzoni L, Matera AG (2008). SMN complex localizes to the sarcomeric Z-disc and is a proteolytic target of calpain. Hum Mol Genet 17, 3399–3410.
Wee CD, Kong L, Sumner CJ (2010). The genetics of spinal muscular atrophies. Curr Opin Neurol 23, 450–458.
Wishart TM, Mutsaers CA, Riessland M, Reimer MM, Hunter G, Hannam ML, Eaton SL, Fuller HR, Roche SL, Somers E, *et al.* (2014). Dysregulation of ubiquitin homeostasis and β-catenin signaling promote spinal muscular atrophy. J Clin Invest 124, 1821–1834.
Ye Y, Rape M (2009). Building ubiquitin chains: E2 enzymes at work. Nat Rev Mol Cell Biol 10, 755–764.
Zhang L, Xu M, Scotti E, Chen ZJ, Tontonoz P (2013). Both K63 and K48 ubiquitin linkages signal lysosomal degradation of the LDL receptor. J Lipid Res 54, 1410–1420.
Zheng N, Schulman BA, Song L, Miller JJ, Jeffrey PD, Wang P, Chu C, Koepp DM, Elledge SJ, Pagano M, *et al.* (2002). Structure of the Cul1-Rbx1-Skp1-F boxSkp2 SCF ubiquitin ligase complex. Nature 416, 703–709.
Zhou R, Silverman N, Hong M, Liao DS, Chung Y, Chen ZJ, Maniatis T (2005). The role of ubiquitination in Drosophila innate immunity. J Biol Chem 280, 34048–34055.